Title: Enhanced protective efficacy of a novel, thermostable, RBD-S2 vaccine formulation against SARS-CoV-2 and its variants

Authors: Nidhi Mittal[1], Sahil Kumar[2], Raju S Rajmani[1], Randhir Singh[3], Céline Lemoine[4], Virginie Jakob[4], Sowrabha BJ[3], Nayana Jagannath[3], Madhuraj Bhat[3], Debajyoti Chakraborty[1], Suman Pandey[3], Aurélie Jory[5], Suba Soundarya S.A.[5], Harry Kleanthous[6], Patrice Dubois[4], Rajesh P. Ringe[2*], Raghavan Varadarajan[1*]

Affiliations:

[1]Molecular Biophysics Unit (MBU), Indian Institute of Science; Bengaluru 560012, India

[2]Virology Unit, Institute of Microbial Technology, Council of Scientific and Industrial Research (CSIR); Chandigarh 160036, India

[3]Mynvax Private Limited; 3rd Floor, Brigade MLR Centre, No.50, Vani Vilas Road, Basavanagudi, Bengaluru 560004, India

[4]Vaccine Formulation Institute; Rue du Champ-Blanchod 4, 1228 Plan-les-Ouates, Switzerland

[5]National Centre for Biological Sciences, Tata Institute of Fundamental Research; Bengaluru 560065, India

[6]Bill and Melinda Gates Foundation; Seattle, WA, 98109, USA

*Corresponding authors: rajeshringe@imtech.res.in ; varadar@iisc.ac.in

Abstract: With the rapid emergence of variants of concern (VOC), the efficacy of currently licensed vaccines has reduced drastically. VOC mutations largely occur in the S1 subunit of Spike. The S2 subunit of SARS-CoV-2 is conserved and thus more likely to elicit broadly protective immune responses. However, the contribution of the S2 subunit in improving the overall efficacy of vaccines remains unclear. Therefore, we designed, characterized, and evaluated the immunogenicity and protective potential of a stabilized SARS-CoV-2 Receptor Binding Domain (RBD) fused to a stabilized S2. Designed immunogens were expressed as soluble proteins with approximately fivefold higher purified yield than the Spike ectodomain and formulated along with Squalene-in-water emulsion (SWE) adjuvant. S2 immunization failed to elicit a neutralizing immune response but significantly reduced lung viral titers in mice challenged with the heterologous Beta variant. In hamsters, SWE-formulated RS2 showed enhanced immunogenicity and efficacy relative to corresponding RBD and Spike formulations. Despite being based on the ancestral Wuhan strain of SARS-CoV-2, RS2 exhibited broad neutralization, including against Omicron variants (BA.1, BA.5 and BF.7), as well as the clade 1a WIV-1 and SARS-CoV-1 strains. RS2 sera also showed enhanced competition with both S2 directed and RBD Class 4 directed broadly neutralizing antibodies, relative to RBD and Spike elicited sera. When lyophilized, RS2 retained antigenicity and immunogenicity even after incubation at 37 °C for a month. The data collectively suggest that the RS2 immunogen is a promising modality to combat SARS-CoV-2 variants.

Keywords: Protein engineering, lyophilization, potency, protein design, COVID-19 vaccine, thermotolerant.

INTRODUCTION

The severe acute respiratory syndrome coronavirus 2 (SARS-CoV-2) virus is the causative agent of the COVID-19 pandemic [1]. A variety of SARS-CoV-2 vaccines were developed at an unprecedented pace to combat the pandemic [2–8]. Spike (S) is a ~ 200 kDa transmembrane glycoprotein composed of two functional subunits: the N-terminal S1 subunit, which mediates attachment to the host receptors, and the C-terminal S2 subunit, which facilitates membrane fusion [9–11]. Spike protein is highly immunogenic, and the receptor-binding domain (RBD) contains the major neutralizing antibody epitopes [12–18]. Most currently approved vaccines are based on the Spike immunogen, and a minority are based on RBD. RBD-based vaccines have been shown to elicit moderate to high-neutralizing antibody titers [19–22]. However, due to rapid virus evolution, various variants of concern (VOC) mutations have been identified primarily in the N-terminal domain (NTD) and RBD of the S1 subunit [23]. These mutations increase viral infectivity and induce immune evasion by evading virus neutralization. Requirements for low or ultracold temperature storage have acted as barriers to vaccine deployment in low-and middle-income countries (LMICs). There is an ongoing need for vaccination in vulnerable sections of the population, including pregnant women, those with co-morbidities and the elderly, both to protect these individuals and to minimize the potential for viral evolution in vulnerable hosts. Therefore, it remains important to develop and test vaccine candidates that confer a potent, protective, humoral immune response to a broad spectrum of SARS-CoV-2 variants and do not require a cold-chain for last mile distribution.

Compared to the S1 subunit, the S2 subunit of coronaviruses is more conserved and likely to elicit broadly protective antibodies [24]. Several cross-reactive monoclonal antibodies against the S2 stem helix region have been identified, and a few of them have been shown to neutralize SARS-CoV-2, thereby conferring *in vivo* protection [17,25–33]. Spike microarray analysis demonstrated that cross-reactive antibodies are elicited against the S2 stem helix region during natural infection [17]. The stem-helix epitope in the S2 region, residues (1142-1165) is well conserved, and antibodies that bind to this region neutralize diverse coronaviruses suggesting that immunogens containing this cryptic epitope might elicit pan-coronavirus immunity.

However, the protective efficacy of S2 as an immunogen remains unclear. It is also known that the bulk of the neutralizing response is directed against the RBD. While there are also neutralizing

antibodies directed against the NTD of the Spike, these have lower breadth than the RBD-directed neutralizing antibodies, as the major NTD neutralizing epitope is mutated in VOCs [34–38].

To address these issues, we designed a stabilized S2-ectodomain, and genetic fusions of a previously designed, stabilized RBD with S2 [39]. These are referred to as RS2 and S2R immunogens depending on the order of connectivity of RBD and S2. Designed RS2 and S2R immunogens were expressed with ~5.3-fold higher purified yield than stabilized Spike ectodomain in mammalian cells. Sepivac SWE™ is an MF59 like oil-in-water emulsion adjuvant, subsequently referred to as SWE. Two immunizations of SWE adjuvanted RS2 induced robust neutralizing immune responses and conferred protection against SARS-CoV-2 variants in mice, showing superior immunogenicity and protective efficacy, compared to stabilized RBD, and comparable immunogenicity to stabilized Spike formulations. In hamsters, RS2 showed superior immunogenicity and protective efficacy to a similarly adjuvanted, stabilized Spike formulation. When lyophilized, RS2 retained antigenicity and immunogenicity even after incubation at 37 °C for a month. The data collectively suggest that RS2 containing vaccine formulations are a promising modality to combat SARS-CoV-2 variants.

RESULTS

Immunogen Design

For designing an S2-based SARS-CoV-2 immunogen, S2 subunit residues interacting with the S1 subunit were identified by accessibility calculations using the Naccess program on PDB 6VXX. Accessible surface areas (ASAs) of all residues in Spike were calculated in the absence and presence of the S1 subunit. Residues of the S2, which had a total side-chain ASA difference of >5 $Å^2$, were identified as S1 interacting residues. The following mutations were made to mask newly exposed hydrophobic residues to prevent S2 aggregation in the absence of S1, namely F855S, L861E, L864D, V976D, and L984Q [40,41].

Proline substitutions in the loop between HR1 (heptad repeat 1) and the central helix in fusion proteins from viruses like SARS-CoV-2, SARS-CoV, MERS-CoV, and RSV are known to retain prefusion conformation, and enhance expression yields [42–45]. More recently, HexaPro Spike, a S-6P variant, with six proline substitutions (F817P, A892P, A899P, A942P, K986P, V987P)

104 displayed 9.8-fold increased protein expression and ~5 °C increase in T_m relative to S-2P (Spike
105 with two proline mutation) [46]. Hence, we additionally included all these six proline substitutions
106 in the present S2 immunogen (S2) comprising residues 698-1211 of the SARS-CoV-2 Spike. Since
107 RBD contains the major neutralizing antibody epitopes on Spike and S2 is well conserved, we
108 designed RS2 and S2R immunogens **(Fig. 1A)**. For this, an S2 fragment comprising residues 698-
109 1163 of the SARS-CoV-2 was genetically fused with our previously reported high-yielding,
110 thermostable RBD containing A348P, Y365W, and P527L mutations [20,22].

111 **Biophysical characterization of S2, RS2, S2R and Spike**

112 The designed immunogens were transiently expressed as secreted proteins in Expi293F
113 suspension cells. Recombinant proteins S2, RS2, and S2R were purified in high yields of ~120
114 mg/L, ~850 mg/L, and ~800 mg/L, respectively, using nickel affinity chromatography **(Fig. 1B)**.
115 The oligomeric state of the immunogens was determined using size exclusion chromatography
116 (SEC), and revealed that S2 exists as homogenous nonamers in the solution **(Fig. 1C)**. RS2 and
117 S2R exist as a mixture of monomers and trimers, and the calculated molecular weights were in
118 good agreement with the theoretical molecular weight **(Fig. 1D, E)**.
119 For comparison, the stabilized trimeric Spike ectodomain (1-1211) containing six proline
120 mutations (F817P, A892P, A899P, A942P, K986P, and V987P), along with the additional three
121 RBD stabilizing mutations (A348P, Y365W, and P527L) described above, was also expressed and
122 purified from Expi293F cells **(Fig 1A, B, F)** with a purified yield of ~150 mg/L [22,46].
123 The apparent melting temperature (T_m) and the thermal unfolding profile of designed immunogens
124 and Spike was determined using Nano-DSF. The RS2 and S2R displayed similar thermal
125 unfolding profiles and comparable T_m of ~ 50 °C **(Fig. 2A and B)**. The S2 immunogen exhibited
126 T_m of 52.2 °C while the stabilized trimeric spike demonstrated two T_m, T_{m1} of 50.4 °C and T_{m2} of
127 61.5 °C, which implied that trimeric Spike has different structural components of varying stability
128 **(Fig. 2C and D).** RS2, S2R, and S2, when subjected to 37 °C for 1 hour, exhibited similar thermal
129 unfolding profiles to those protein samples stored at 4°C **(Fig. 2E-G)**. However, the Spike showed
130 a slightly broadened thermal unfolding profile after incubation at 37 °C, with more noticeable
131 broadening at 50°C **(Fig. 2H)**. Moreover, RS2 and S2R were found to be stable even after
132 incubation at 50°C, although a slight decrease was observed. On the other hand, S2 was thermally
133 unstable at 50°C, which suggested that RS2 and S2R are more resistant to transient thermal stress

134 than Spike and S2. **(Fig. 2E-H)**. Compared to the other designed immunogens and Spike, RS2
135 was more rapidly digested by TPCK-trypsin at both 4 °C and 37 °C, (**Fig. 2H-K).** This data
136 suggested that RS2 is more susceptible to proteolytic degradation than S2R, S2, and Spike, which
137 showed highest proteolytic stability. Whether the apparent enhanced proteolytic resistance of
138 Spike **(Fig. 2L)** is due to aggregation following initial proteolytic cleavage, remains to be
139 elucidated.

140 The binding of S2, RS2, and S2R immunogens to its cognate receptor, ACE2-hFc, a panel of RBD
141 conformation-specific (CR3022, S309, ADG-2, and H014) and S2-specific (B6 and CC40.8)
142 antibodies were probed using surface plasmon resonance (SPR). Spike, RS2, and S2R bound well
143 with ACE2-hFc, RBD-specific, and S2-specific antibodies **(Table 1 and 2)**. S2 binds only to S2-
144 specific antibodies with high affinity. This indicated the proper folding of designed immunogens
145 **(Table 2)**.

146 **Immunogenicity and protective efficacy of S2R relative to S2 and RBD immunogens against**
147 **heterologous challenge.**

148 Since in the initial characterizations, S2R showed higher proteolytic stability and comparable
149 thermal stability to RS2, the immunogenicity and protective efficacy of S2R, relative to RBD and
150 S2 immunogens, was evaluated in hACE-2 expressing C57BL/6 transgenic mice. Our previously
151 reported mammalian cell expressed, stabilized RBD containing A348P, Y365W, and P527L
152 mutations was expressed and purified [20,22]. Mice were intramuscularly immunized with 2 µg
153 immunogens (S2R, S2 or RBD) formulated with SWE in a prime-boost regimen 3 weeks apart.
154 SWE is equivalent to MF59, a very safe adjuvant that has been used for many years in the context
155 of human influenza vaccines [47]. While there are other more potent adjuvants available, stronger
156 adjuvant mediated immune responses can be associated with unfavorable side effects [47]. Two
157 weeks post-boost, RBD, S2 and Spike-specific IgG titers in sera of immunized mice were
158 measured using ELISA. Relative to RBD and S2, the S2R immunogen elicited significantly higher
159 RBD, S2 and Spike-specific ELISA endpoint titers **(Fig. 3A-C)**. S2R immunized mice elicited
160 significantly higher neutralizing antibody titers against B.1 pseudovirus compared to RBD
161 immunized mice, while the sera from S2 immunized mice failed to neutralize B.1 pseudovirus
162 **(Fig. 3D)**. At this administered dose, sera from RBD-immunized mice did not show neutralization

163 against BA.1. However, S2R immunized mice sera showed neutralization against BA.1, BA.5, and
164 BF.7 albeit at significantly reduced levels **(Fig. 3E and F)**. Furthermore, these sera exhibited
165 substantial cross-neutralization against heterologous clade1a SARS-CoV-1 viruses, which
166 demonstrates the potential of S2R to elicit broadly protective antibodies against sarbecoviruses
167 **(Fig. 3F)**. Although the neutralization ID_{50} was too low to be measured in mice immunized with
168 SWE formulated S2**,** addition of these S2 elicited sera enhanced neutralization potency of the
169 broadly neutralizing antibody S309 **(Fig. 3G)**.

170 Next, the protective efficacy of RBD, S2, and S2R formulations was assessed against the Beta
171 variant of SARS-CoV-2. Unimmunized-unchallenged, and unimmunized-Beta variant challenged
172 mice were used as control groups. Three weeks post boost, mice were intranasally challenged with
173 10^5 plaque-forming units (pfu) of Beta variant virus, and weight change was monitored for upto
174 five days. Only 33% of unimmunized mice survived, while 72% of S2 immunized mice survived
175 Beta-variant challenge. In contrast, all RBD and S2R immunized mice survived the Beta variant
176 challenge **(Fig. 3H)**. Post challenge, no weight change was seen in S2R immunized mice. Mice
177 immunized with RBD, and S2 showed a significant weight reduction of ~10 % and ~17%
178 respectively. As expected, no weight reduction was observed in the unimmunized group, while 22-
179 25 % weight reduction was seen in the unimmunized-Beta variant challenged group **(Fig. 3I)**. Mice
180 immunized with either RBD, S2 or S2R showed significantly lower lung viral titers than
181 unimmunized mice challenged with the Beta variant **(Fig. 3J)**. Despite lack of neutralization, lung
182 viral titers were significantly reduced in the S2-immunized group, suggesting that S2 provides
183 protection by non-neutralizing mechanisms. The lung tissue sections obtained from S2R
184 immunized mice showed clear interstitial spaces within lung epithelium and reduced immune cell
185 infiltration compared to unimmunized-Beta variant challenged group, RBD and S2 immunized
186 group **(Fig. 3K and L)**.

187 **RS2 is more immunogenic than S2R in mice.**

188 At the same time, we also compared the immunogenicity of RS2 and S2R in BALB/c mice.
189 BALB/c mice were vaccinated twice intramuscularly with either 20 μg of RS2 or S2R formulated
190 with SWE adjuvant. Two weeks after the second vaccination, RBD and Spike specific IgG titers
191 and neutralizing immune responses were measured in the sera samples of immunized mice. Both
192 RS2 and S2R immunized mice elicited equivalent RBD and Spike-specific ELISA endpoint titers

193 **(Fig. S1 A and B).** RS2 elicited significantly higher neutralizing titers against B.1 pseudovirus
194 **(Fig. S1C)**. Neutralizing titers against Delta variant were also higher in RS2 immunized mice sera
195 but differences did not reach statistical significance **(Fig. S1D)**. Thus, the data indicated that RS2
196 is more immunogenic than S2R. Hence for all further studies, including formulation stability and
197 comparative immunization studies with Spike, RS2 was used.

198 **RS2 induces an equivalent neutralizing immune response to Spike ectodomain in mice and**
199 **protects against mouse-adapted SARS-CoV-2 challenge.**

200 Considering that most currently licensed COVID-19 vaccines have the Spike as the sole
201 immunogen, we compared the immunogenicity and protective efficacy of RS2 with the stabilized
202 Spike ectodomain. BALB/c mice were intramuscularly immunized with 2 µg of RS2 or Spike
203 formulated with SWE adjuvant in a prime-boost regimen 21 days apart. Fourteen days post-second
204 immunization, both RS2 and Spike immunized mice elicited high RBD, S2 and Spike-specific IgG
205 titers **(Fig. 4A-C)**. Although the neutralizing titers against B.1, Beta and Delta variant
206 pseudoviruses were comparatively higher in RS2 immunized mice sera than Spike immunized
207 mice sera, the differences did not reach statistical significance **(Fig. 4D-F)**. Sera from RS2 and
208 Spike immunized mice also showed neutralization against BA.1, BA.5 and BF.7 pseudoviruses,
209 albeit with lower titers **(Fig. 4G-I)**. Compared to Spike, RS2 also exhibited substantial cross-
210 neutralization against heterologous clade1a SARS-CoV-1 and WIV-1 viruses, which demonstrates
211 the potential of RS2 to elicit broadly protective antibodies against sarbecoviruses **(Fig. 4J and K)**.
212 Three weeks post-boost, all mice were intranasally challenged with 10^5 pfu of mouse-adapted
213 SARS-CoV-2 MA10 virus. One-day post-challenge, mice immunized with either RS2 or spike
214 showed a slight body weight reduction of ~5 %, and from day two, all mice regained their initial
215 weight. In contrast, unimmunized-MA10 challenge control mice showed ~25 % weight loss by
216 day four, post-challenge. No weight change was seen in the unimmunized-unchallenged control
217 group **(Fig. 4L)**. RS2 and Spike immunized mice showed significantly reduced lung viral titers
218 compared to unimmunized-MA10 mice **(Fig. 4M)**. Analysis of lung tissue sections of mice
219 immunized with RS2 showed clear lung epithelial interstitial spaces and lower immune cell
220 infiltration compared to both Spike immunized and unimmunized MA10 challenged group **(Fig.**
221 **4N and O)**. This data suggests that RS2 elicits a broadly neutralizing humoral immune response
222 and protects against SARS-CoV-2 MA10 virus challenge.

223 **Thermal stability of RS2**

224 As with our previously reported RBD immunogens, our newly designed RS2 immunogen showed
225 identical thermal unfolding profiles before and after lyophilization and solubilization, suggesting
226 that lyophilization did not affect the thermal stability of these immunogens **(Fig. S2A)** [20,22].
227 Further, the effect of transient thermal stress on the thermal stability of lyophilized RS2 was
228 studied by performing nano-DSF. Following incubation at different temperatures (4 °C, 37 °C, 50
229 °C, 70 °C and 90 °C) for 60 min, no change in thermal unfolding profiles was observed **(Fig. S2B)**.
230 Moreover, the T_m and conformational integrity of lyophilized RS2 protein remained unchanged
231 after a month of storage at 37 °C **(Fig. S2C) (Table 3)**. In addition, the antigenicity of RS2 was
232 assessed by performing SPR using a panel of RBD and S2-specific antibodies. Interestingly,
233 following thermal stress, RS2 retained binding with the cognate receptor ACE2-hFc, RBD-
234 specific antibodies (CR3022, S309), and S2-specific antibodies (B6, CC40.8). This suggests that
235 lyophilized RS2 immunogen is resistant to transient thermal stress **(Fig. S2D-H)**. The stability of
236 SWE adjuvanted RS2 in PBS buffer was also evaluated at 5 °C and 40 °C over a period of one
237 month. Antigen integrity and physiochemical characterization of SWE adjuvanted RS2
238 formulations was carried out by performing ELISA, particle size, polydispersity, zeta potential,
239 pH, osmolality and squalene content measurements. The RS2 formulation in SWE is stable at 5°C
240 and 40 °C in both polypropylene tubes and glass vials for at least one month **(Fig. 5A-K)**.

241 **Protective efficacy of lyophilized RS2 formulation after month long storage at 37 °C**

242 The immunogenicity of the lyophilized RS2 protein stored at 37 °C for a month was evaluated in
243 hACE-2 expressing C57BL/6 transgenic mice. Mice were intramuscularly immunized with 20 µg
244 immunogen extemporaneously formulated with SWE adjuvant in a prime-boost regimen. Two
245 weeks following the boost, the formulation showed high RBD, S2 and Spike-specific binding
246 titers, and neutralizing titers against B.1, Beta, Delta, and BA.1 pseudoviruses **(Fig. 6A and B)**.
247 The above formulation elicited equivalent neutralization titers to a non-lyophilized freshly
248 prepared RS2 formulation stored at 4 °C, against B.1 and BA.1 pseudoviruses **(Fig. 6C)**. Twenty-
249 one days following the boost, mice were challenged with 10^4 pfu of Beta and Delta variants of
250 SARS-CoV-2. None of the unimmunized control mice survived Beta variant challenge, while 57%
251 of unimmunized control mice survived Delta variant challenge and the remaining mice showed 20

% weight loss, nine days post-challenge. In contrast, all RS2 immunized mice survived the Beta and Delta variant SARS-CoV-2 challenges and showed no weight loss **(Fig. 6D-F)**. Lung viral titers of RS2-immunized mice challenged with Beta and Delta variants were below the detection limit and lung tissues showed minimal pathology **(Fig. 6G and H).** Lung viral titers and tissue sections from the unimmunized mice challenged with the Beta variant were not examined because none of the mice survived. These findings indicate that RS2 is stable and immunogenic even after storage at 37 °C for at least one-month.

RS2 shows superior immunogenicity and protective efficacy to stabilized Spike ectodomain in hamsters.

Protective efficacy of RS2 was compared with the stabilized Spike against challenge with the Beta variant of SARS-CoV-2 in Syrian hamsters. Female Syrian Golden hamsters were immunized with 5μg of stabilized Spike or RS2 formulated with SWE on day 0 and day 21, while the control group of hamsters was immunized with SWE adjuvant in PBS. Both Spike and RS2 immunized hamsters elicited high RBD, S2 and Spike-specific ELISA endpoint titers **(Fig. 7A-C)**. Notably, two immunizations with 5 μg SWE adjuvant formulated RS2 elicited significantly higher neutralizing titers against B.1, Beta, Delta and Omicron BA.1, BA.5 and BF.7 variants than corresponding titers elicited by SWE formulated Spike in hamsters **(Fig. 7D-I)**. Consistent with the BALB/c mice study, RS2 immunized hamsters exhibited substantially higher cross-neutralizing activity against clade 1a sarbecoviruses, WIV-1 and SARS-CoV-1 compared to those of Spike immunized hamsters (**Fig. 7H and K)**. Moreover, hamsters immunized with RS2 showed initial transient weight loss (up to 3 %) and regained weight at 3 days post Beta variant infection. In contrast, Spike-immunized hamsters showed comparatively higher lung viral titers and weight loss, while no weight regain was observed **(Fig. 7L and M)**. Both RS2 and Spike immunized hamsters showed significantly reduced lung viral titers compared to unimmunized-Beta challenged hamsters **(Fig. 7M)**. Analysis of RS2 and Spike immunized hamster lung tissue sections showed clear lung epithelial interstitial spaces and lower immune cell infiltration compared to the unimmunized Beta-challenged groups **(Fig. 7N and O)**. Overall, the data shows that RS2 is more immunogenic and efficacious than Spike in hamsters.

DISCUSSION

281 Vaccination has significantly reduced the global health burden caused by the COVID-19
282 pandemic. While vaccines have been proven to be highly efficacious against ancestral SARS-CoV-
283 2 stain, their efficacy has rapidly declined against new VOCs and periodic updating of vaccines
284 appears to be necessary. Most VOC mutations are identified in the receptor binding motif (RBM)
285 region of RBD. The substantial waning of serum-neutralizing antibody titers and the emergence
286 of variants with increased transmissibility and neutralizing antibody escape responses are
287 associated with increased breakthrough infection in vaccinated individuals. To curb infection and
288 sustain vaccine effectiveness, booster doses are required.

289 Various approaches have been deployed to broaden the protection breadth of SARS-CoV-2
290 vaccines, which include mosaic nanoparticle vaccine designs that display multiple RBDs from
291 different sarbecoviruses, and conferred broad protection against diverse coronaviruses, albeit with
292 a reduction in potency against some SARS-CoV-2 VOCs [48–50]. While promising, such nanoparticle
293 vaccine designs elicit titers against the nanoparticle scaffolds, and employ a large number of
294 antigens, which adds to manufacturing complexity. Alternatively, vaccine candidates based on
295 conserved antigens like S2 are also reported [51–53].

296 In the present study we designed a stabilized S2 ectodomain, and the genetic fusion of RBD and
297 S2. The RS2 and S2R contain the RBD component to elicit potent neutralizing antibodies, and the
298 S2 to increase immunogenicity and protective breadth. The novel RS2 and S2R immunogens
299 exhibited ~5.3-fold higher protein yields and were shown to be more stable to transient thermal
300 stress than a stabilized Spike **(Fig. 2E and H)**.

301 All the currently licensed COVID-19 vaccines require refrigerated or frozen storage. Recently,
302 Ferritin displayed, alum adjuvanted Spike construct also displayed promising immunogenicity in
303 non-human primates and could be stored at 37°C for at least two weeks[54]. In the present study we
304 have shown that our RS2 vaccine candidate can retain its thermal stability and antigenicity without
305 any loss of immunogenicity and protective efficacy at 37 °C for at least a month. Encouragingly,
306 RS2 immunogen formulated with SWE was also shown to maintain its physico-chemical stability
307 at 40°C for up to one month, however the immunogenicity needs to be evaluated. This exceptional
308 stability of the RS2 candidate will facilitate distribution in low resource settings and will reduce
309 the cost associated with low or ultracold temperature storage and transportation.

310 Despite being based on the original Wuhan strain sequence, RS2 elicited neutralizing antibodies
311 against B.1, Beta, Delta, Omicron (BA.1, BA.5, BF.7) and clade 1a SARS-CoV-1 and WIV-1
312 pseudoviruses in mice and hamsters. While many SARS-CoV-2 immunogens exhibit high
313 immunogenicity in mice, immunogenicity is poorer in hamsters, and more predictive of
314 immunogenicity in humans[55–58]. Therefore, we chose to use the hamster animal model to further
315 probe for apparent differences in immunogenicity between RS2 and Spike immunized animals. In
316 hamsters, the RS2 immunogen elicited significantly higher neutralizing titers against all the tested
317 VOCs compared to Spike **(Fig.7D-K)**. Qualitatively, RS2 immunized animals also exhibited less
318 weight loss and lower lung viral titers compared to Spike immunized animals **(Fig.7H-J)**.
319 However, due to the limited number of animals in the study, the differences in weight loss and
320 lung viral titers between the two groups did not reach statistical significance. In addition, the sera
321 obtained from mice immunized with RS2 showed competition with S2X259, and B6 antibodies.
322 In contrast, the sera from mice immunized with Spike or RBD failed to show competition with
323 these antibodies **(Fig. S3)**. These findings suggest that RS2 sera specifically target highly
324 conserved epitopes located in the RBD and S2 stem helix, which are likely less accessible in Spike
325 or RBD based immunogens. In contrast to Spike where regions of RBD that contain neutralizing
326 epitopes are occluded in the down conformation, there no such conformational constraint in the
327 RBD-S2 fusions.

328 Like other vaccine formulations, it will be necessary to periodically update formulations based on
329 RS2. However, due to the lower mutation rate in the S2 region and higher yield, updating RS2
330 vaccine sequences to match circulating vaccines is expected to be easier than updating full length
331 Spike based vaccines.

332 In contrast to RS2, the S2 component alone induces high IgG binding titers but sera failed to
333 neutralize the viruses[52,53]. Addition of S2-elicited sera significantly enhanced neutralization
334 potency of the RBD directed, broadly neutralizing S309 antibody **(Fig. 3G).** This finding further
335 supports the role of S2 in boosting immunogenicity and enhancing the protective efficacy of the
336 vaccine designs based on genetic fusion of RBD and S2 as in RS2 and S2R.

337 Similar to previous reports, our study reaffirms that despite lack of significant neutralization titers,
338 lung viral titers were significantly reduced in S2 immunized animals. This indicates that either T-

339 cell mediated or S2 directed antibodies, could offer protection through non-neutralizing
340 mechanisms, but these were not evaluated in the present study. In future, further characterization
341 of cellular immune responses and the effector functions of S2 directed antibodies will be evaluated,
342 to provide insights into the diverse mechanisms underlying the observed reduction in viral loads.

343 In conclusion, our study demonstrates that RS2 has several advantages compared to Spike, based
344 on its improved immunogenicity in small animals, higher thermal tolerance, and substantially
345 greater purified yield. Currently a significant proportion of the world's population has been
346 immunized with vaccines with full-length Spike immunogens, and likely an even larger number
347 of people have acquired natural immunity through infection. In this scenario an RS2 vaccine could
348 still be used as a booster vaccine in vulnerable groups that will require annual vaccination and
349 could also be combined with other vaccine formulations for respiratory viruses. Given that the
350 virus is likely to continue to circulate in humans for the foreseeable future, it is important to
351 continue developing and improving vaccine technologies both to combat this evolving virus and
352 for future preparedness against other coronavirus pandemics. The RS2 vaccine design can be used
353 as a prototype for designing vaccines that target other coronaviruses, or potential future variants
354 of SARS-CoV-2.
355

356 **MATERIALS AND METHODS**

357 **Expression and Purification of recombinant proteins**

358 Designed immunogens S2, RS2, S2R and Spike are based on the ancestral Wuhan SARS-CoV-2
359 strain (GenBank Id: YP_009724390.1). Mammalian codon optimized genes for S2, RS2 and S2R
360 were synthesized at GenScript Inc. The designed immunogens consisted a HRV3C protease site
361 (LEVLFQGP) at the C-terminus of proteins to facilitate histidine tag removal after purification.
362 Recombinant proteins S2, RS2, S2R, RBD, and Spike were transiently expressed in Expi293F™
363 cells according to the manufacturer's guidelines (Gibco, ThermoFisher Scientific). Briefly,
364 Expi293F™ cells were maintained at a cell density of ~3×10^6 viable cells/mL in the Expi293F™
365 expression medium. Plasmid DNA and ExpiFectamine™ 293 reagent were diluted with Opti-
366 MEM™ I reduced serum media and incubated at room temperature for 5 min. After 15-20 min,
367 ExpiFectamine™ 293/Plasmid DNA complexes were slowly added to Expi293F™ cells. Eighteen
368 hours post-transfection, ExpiFectamine™ 293 Transfection Enhancer 1 and 2 were added to the
369 transfected cells. Six days post-transfection, culture was harvested, and proteins were purified from
370 culture supernatant by nickel affinity chromatography. The culture supernatant was incubated with
371 Ni-Sepharose 6 Fast Flow resin (GE Healthcare) for 6-8 h at 4 °C. Non-specific proteins were
372 removed by passing twenty-column volumes of wash buffer (PBS containing 25 mM Imidazole,
373 pH 7.4). Bound proteins were eluted from the Ni-NTA column using 500 mM imidazole in PBS
374 buffer, pH 7.4, and were dialyzed against PBS buffer using a 10 kDa (MWCO) dialysis membrane.
375 The purity of purified protein samples was analyzed on SDS-PAGE.

376 **Size Exclusion Chromatography (SEC)**

377 A Superdex-200 10/300 analytical column, equilibrated with PBS buffer, pH 7.4, was used for size
378 exclusion chromatography-multi angle light scattering. 100-200 µg of purified protein samples
379 were injected into the column, and protein peaks were resolved on a BioRad NGC chromatography
380 system at a flow rate of 0.4 mL/min.

381 **Differential Scanning Fluorimetry (nano-DSF)**

382 A Prometheus NT.48 instrument was used to determine the thermal stability of immunogens. The
383 thermal unfolding of immunogens was monitored from 20 °C to 95 °C at a scan rate of 1 °C/min
384 [59].

385 **Trypsin Proteolysis**

386 The proteolytic stability of designed immunogens was studied by performing trypsin proteolysis.
387 S2, RS2, and S2R were dialyzed against 50 mM Tris buffer (pH 7.5) containing 1 mM $CaCl_2$,
388 followed by incubation with TPCK trypsin (protease) in a 1:50 molar ratio at 4 °C and 37 °C. At
389 different time points, aliquots were taken out, and the reaction was quenched using 6X-SDS-
390 loading dye. Collected samples were analyzed on 12 % SDS-PAGE.

391 **Surface Plasmon Resonance (SPR)**

392 The binding affinity of the S2, RS2, S2R and Spike immunogens to different RBD and S2-specific
393 antibodies were measured using ProteOn XPR36 Protein Interaction Array V.3.1. The SPR sensor
394 prism HC200M chip (Xantec bioanalytics) was first activated with EDC and sulfo-NHS. Then
395 Protein G (10 µg/mL) was immobilized in the presence of 10 mM sodium acetate buffer, pH 4.0.
396 Finally, excess sulfo-NHS esters were quenched using 1 M ethanolamine. 500 response units
397 (R.U.) of ACE2-hFc, RBD specific monoclonal antibodies: CR3022, S309, ADG-2, H014, and
398 S2-specific monoclonal antibodies: B6 and CC40.8 were immobilized. Different protein sample
399 concentrations (100 nM, 50 nM, 25 nM, 12.5 nM, and 6.25 nM) were passed over the HC200M
400 chip surface at a flow rate of 30 µL/min, followed by dissociation with PBS buffer containing
401 0.05% tween-20 (PBST). After each kinetic-binding assay, the chip was regenerated using 0.1 M
402 Glycine-HCl, pH 2.7. Proteon Manager was used for fitting data to a simple 1:1 Langmuir
403 interaction model to obtain kinetic parameters.

404 **Formulation preparation with SWE adjuvant**

405 The adjuvant SWE (squalene-in-water emulsion) was co-developed by the Vaccine Formulation
406 Institute (Switzerland) and Seppic (France) and is available at GMP grade (Sepivac SWE™) under
407 an open access model. Immunogens (S2, S2R or RS2) were formulated with SWE at 1:1 volume
408 ratio. The formulation RS2 in combination with SWE was evaluated for 1 month stability
409 measuring adjuvant physicochemical characteristics and antigen integrity. Measurements
410 included: visual inspection, particle size and polydispersity (DLS), zeta potential (ELS), pH,
411 osmolality, and squalene content (HPLC). Antigen integrity was evaluated by ELISA.

412 **Immunization Studies**

413 *(BALB/c mice immunizations):* Groups of 6-8 weeks old, female BALB/c mice (n=5) were
414 intramuscularly immunized with either 2 µg or 20 µg dose of SWE adjuvant formulated RS2
415 immunogen.
416 *(hACE-2 expressing C57BL/6 transgenic mice immunizations):* Groups of hACE-2 expressing
417 transgenic mice (n=6/7) were intramuscularly immunized with 2 µg and/or 20 µg dose of SWE
418 adjuvant formulated immunogens (S2, RS2, S2R, Spike, and RBD). B6N; DBA2-Tg(K18-
419 hACE2)3068Mgef/Blisc (acrc:21000509) mice strain was generated and provided by the Mouse
420 Genome Engineering Facility, NCBS Bangalore using the K18-hACE2 transgene plasmid, kindly
421 donated by Dr Paul B. McCray [60]
422 *(Syrian Hamster Immunizations):* Groups of five female golden Syrian hamsters were
423 intramuscularly immunized with either a 5 µg or 20 µg dose of SWE adjuvant-formulated
424 immunogens (RS2, Spike, and RBD).

425 SWE adjuvant-treated animals were used as control. The sera samples from immunized and
426 unimmunized animals were collected before prime (Day -1), 2 weeks post-prime (Day 14), and 14
427 days post-boost (Day 35) for endpoint ELISA and measuring neutralizing antibody titers.
428 *Challenge Studies:* Twenty-one days following boost immunizations, immunized animals were
429 intranasally challenged with either 10^5 pfu MA10, 10^5 pfu/ 10^4 pfu Beta, or 10^4 pfu Delta VOCs.
430 The unimmunized challenged animals were used as control. Weight change of immunized-
431 challenged animals, unimmunized-unchallenged animals (Unimmunized), and unimmunized-
432 virus challenged control groups were monitored and recorded for 5-9 days. Post-challenge, lungs
433 were harvested for viral titer estimation and histopathological examination were obtained on day
434 6 except for the lyophilized RS2 study, where lung samples were obtained on day 10, as previously
435 described [21]. For lung tissue histopathology scoring, we developed a scientific method using
436 Mitchison's virulence scoring system with some modifications, considering the consolidation of
437 lungs, severity of bronchial and alveolar inflammation, immune cell influx, and alveolar and
438 perivascular edema [21,61]. The histopathology scores were graded as 0-4 (4: Severe pathology; 3:
439 Moderate pathology; 2: mild pathology; 1: Minor/minimum pathology; 0: No pathology).

440 **ELISA and Competition ELISA**

441 As described previously, endpoint titers of serum-binding antibodies were determined using
442 ELISA [22]. Briefly, 96 well ELISA plates were coated with 4 µg/mL RBD (332-532 a.a) or Spike
443 (1-1208 a.a) and incubated at 25 °C for 2-3 h. Plates were washed with PBST, followed by
444 incubation and with blocking with 3 % skimmed milk (in PBST) at 25 °C for 1 h. Four-fold serially
445 diluted antisera raised against immunogens were added to wells and incubated at 25 °C for 1 h.
446 Following three washes with PBST, plates were incubated with 1:5000 diluted goat ALP-
447 conjugated anti-mouse IgG secondary antibody at 25 °C for 1 h. Plates were washed thrice with
448 PBST and incubated with pNPP liquid substrate at 37 °C for 30 min. Optical density (O.D.) was
449 measured at 405 nm. The ELISA endpoint titers were determined as the highest sera dilution with
450 an O.D. signal above 0.2 at 405 nm. Competition ELISA was performed as previously described
451 [22]. Briefly, 96 well plates (HIMEDIA, Cat# EP2-5X10NO) were coated with Expi293 cell
452 produced RS2 at 4 µg/mL concentration in 1x PBS (60 µl/well) and incubated for 2 h at 25 °C
453 under gentle shaking condition (300 rpm) on a thermomixer (Eppendorf, USA) and then plate was
454 transferred to 4 °C cold room for overnight. Next day each well was washed with of 1xPBST
455 (200µl/well) and then treated with blocking solution (100 µL 3% skimmed milk in 1xPBST) for
456 45 min at 25 °C, 300 rpm. The sera isolated from 5 animals in a group were used. Individual sera
457 against the mentioned antigens were added at 2-fold serial dilution with a starting dilution of 1:25
458 in blocking solution (60µL). Only blocking solution was added to the control wells. The plates
459 were then incubated for 1 h at 25°C, 300 rpm. Plates were provided with 3 additional washes with
460 1xPBST (200 µL of 1xPBST/well). An additional blocking step was also performed for 45 min
461 with blocking solution (100µL) incubated at 25°C, 300rpm. An excess of monoclonal antibody
462 either S2X259, or B6 were added (60µL at 20µg/mL) to their respective wells and incubated for
463 one hour at 25°C, 300rpm. Next, three washes were given (200 µL of PBST/well) to remove excess
464 unbound proteins. 50 µl/well Goat Anti-Human IgG Antibody, Alkaline Phosphatase conjugate
465 (Sigma-Aldrich Cat # AP112A, Lot # 3519874; diluted 1:5000 in blocking buffer) was added and
466 samples incubated for 1 hour at 25°C, 300 rpm. Plates were washed 3 times with 200 µL of
467 PBST/well. Finally, 50 µL/well of a 37 °C prewarmed alkaline phosphatase yellow (pNPP) liquid
468 substrate (Sigma-Aldrich, Cat # P7998, Lot # SLCJ1764) was added, and plates were incubated
469 for 30 minutes at 37 °C, 300 rpm. The chromogenic signal was measured at 405 nm using an
470 ELISA plate reader (Emax-Plus Microplate reader, Molecular Devices).

471 The percent competition was calculated using the following equation.

472 $$\% \text{ Competition} = \frac{[\text{Absorbance control} - \text{ Absorbance Sera dilution}]}{[\text{Absorbance control}]} \text{ X } 100$$

473 where**,** *Absorbance control* is the absorbance at 405nm of ACE2-hFc, S2X259 or B6
474 protein/Antibody binding directly to RS2 protein in the absence of sera**,** Absorbance *sera dilution*
475 is the absorbance where the serum dilution is incubated with competitor agents like S2X259 or B6
476 protein. The % competition as a function of serum dilution was fit using a three-parameter
477 nonlinear least squares fit curve using Graph Pad Prism 10.0. The sera dilution at 50 % competition
478 on the fitted curve was termed as the IC_{50} competition titer.

479 **Pseudoviral neutralization assay**

480 Psuedoviral neutralization assays were performed as previously described [21]. The genes encoding
481 Spike proteins from VOC were synthesized at GenScript (USA) except for the SARS-CoV-1
482 pseudovirus which was obtained from Dr Kalpana Luthra at the All India Institute of Medical
483 Sciences, New Delhi. Pseudovirus neutralization titers (ID_{50}) were defined as the serum dilution
484 at which the infectivity of the virus is reduced to 50%.

485 **Statistical Analysis:**
486 Data analysis was performed using GraphPad Prism software 10.0.0. The ELISA binding,
487 neutralization titers, and pseudoviral virus neutralization titer data were analyzed with a two-tailed
488 Mann–Whitney test and non-parametric Kruskal–Wallis with Dunn's multiple, respectively.
489 Weight changes in mice and hamsters were analyzed with a two-tailed Student's t-test. (* indicates
490 $p < 0.05$, ** indicates $p < 0.01$, *** indicates $p < 0.001$, **** indicates $p < 0.0001$).

491 All mice and Hamster immunization studies were approved by the Institutional Animal Ethics
492 Committee (CAF/ETHICS/847/2021; CAF/ETHICS/887/2022). These were carried out at the
493 Central Animal Facility (CAF), Indian Institute of Science, according to CPCSEA and ARRIVE
494 guidelines.

495

496 **REFERENCES**

497 1. Li, Q. *et al.* Early Transmission Dynamics in Wuhan, China, of Novel Coronavirus–Infected
498 Pneumonia. *New England Journal of Medicine* **382**, 1199–1207 (2020).
499 2. Xia, S. *et al.* Effect of an Inactivated Vaccine Against SARS-CoV-2 on Safety and
500 Immunogenicity Outcomes: Interim Analysis of 2 Randomized Clinical Trials. *JAMA* **324**,
501 951–960 (2020).
502 3. Jackson, L. A. *et al.* An mRNA Vaccine against SARS-CoV-2 — Preliminary Report. *New*
503 *England Journal of Medicine* **383**, 1920–1931 (2020).
504 4. Keech, C. *et al.* Phase 1–2 Trial of a SARS-CoV-2 Recombinant Spike Protein Nanoparticle
505 Vaccine. *New England Journal of Medicine* **383**, 2320–2332 (2020).
506 5. Logunov, D. Y. *et al.* Safety and immunogenicity of an rAd26 and rAd5 vector-based
507 heterologous prime-boost COVID-19 vaccine in two formulations: two open, non-
508 randomised phase 1/2 studies from Russia. *Lancet* **396**, 887–897 (2020).
509 6. Zhang, Y. *et al.* Safety, tolerability, and immunogenicity of an inactivated SARS-CoV-2
510 vaccine in healthy adults aged 18–59 years: a randomised, double-blind, placebo-controlled,
511 phase 1/2 clinical trial. *Lancet Infect Dis* **21**, 181–192 (2021).
512 7. Zhu, F. C. *et al.* Safety, tolerability, and immunogenicity of a recombinant adenovirus type-
513 5 vectored COVID-19 vaccine: a dose-escalation, open-label, non-randomised, first-in-
514 human trial. *The Lancet* **395**, 1845–1854 (2020).
515 8. Walsh, E. E. *et al.* Safety and Immunogenicity of Two RNA-Based Covid-19 Vaccine
516 Candidates. *New England Journal of Medicine* **383**, 2439–2450 (2020).
517 9. Walls, A. C. *et al.* Structure, Function, and Antigenicity of the SARS-CoV-2 Spike
518 Glycoprotein. *Cell* **181**, 281-292.e6 (2020).
519 10. Shang, J. *et al.* Cell entry mechanisms of SARS-CoV-2. *Proc Natl Acad Sci U S A* **117**,
520 11727–11734 (2020).
521 11. Wang, Q. *et al.* Structural and Functional Basis of SARS-CoV-2 Entry by Using Human
522 ACE2. *Cell* **181**, 894-904.e9 (2020).
523 12. Barnes, C. O. *et al.* SARS-CoV-2 neutralizing antibody structures inform therapeutic
524 strategies. *Nature* **588**, 682–687 (2020).

525 13. Wu, Y. *et al.* A noncompeting pair of human neutralizing antibodies block COVID-19 virus
526 binding to its receptor ACE2. *Science* **368**, 1274–1278 (2020).
527 14. Huo, J. *et al.* Neutralization of SARS-CoV-2 by Destruction of the Prefusion Spike. *Cell*
528 *Host Microbe* **28**, 445-454.e6 (2020).
529 15. Pinto, D. *et al.* Cross-neutralization of SARS-CoV-2 by a human monoclonal SARS-CoV
530 antibody. *Nature* **583**, 290–295 (2020).
531 16. Brouwer, P. J. M. *et al.* Potent neutralizing antibodies from COVID-19 patients define
532 multiple targets of vulnerability. *Science* **369**, 643–650 (2020).
533 17. Wang, C. *et al.* A conserved immunogenic and vulnerable site on the coronavirus spike
534 protein delineated by cross-reactive monoclonal antibodies. *Nat Commun* **12**, 1–15 (2021).
535 18. Rogers, T. F. *et al.* Isolation of potent SARS-CoV-2 neutralizing antibodies and protection
536 from disease in a small animal model. *Science* **369**, 956–963 (2020).
537 19. Thuluva, S. *et al.* Evaluation of safety and immunogenicity of receptor-binding domain-
538 based COVID-19 vaccine (Corbevax) to select the optimum formulation in open-label,
539 multicentre, and randomised phase-1/2 and phase-2 clinical trials. *EBioMedicine* **83**,
540 104217 (2022).
541 20. Malladi, S. K. *et al.* Design of a highly thermotolerant, immunogenic SARS-CoV-2 spike
542 fragment. *Journal of Biological Chemistry* **296**, 100025 (2021).
543 21. Malladi, S. K. *et al.* Immunogenicity and Protective Efficacy of a Highly Thermotolerant,
544 Trimeric SARS-CoV-2 Receptor Binding Domain Derivative. *ACS Infect Dis* **7**, 2546–2564
545 (2021).
546 22. Ahmed, S. *et al.* A Stabilized, Monomeric, Receptor Binding Domain Elicits High-Titer
547 Neutralizing Antibodies Against All SARS-CoV-2 Variants of Concern. *Front Immunol* **12**,
548 5214 (2021).
549 23. Harvey, W. T. *et al.* SARS-CoV-2 variants, spike mutations and immune escape. *Nat Rev*
550 *Microbiol* **19**, 409–424 (2021).
551 24. Ng, K. T., Mohd-Ismail, N. K. & Tan, Y.-J. Spike S2 Subunit: The Dark Horse in the Race
552 for Prophylactic and Therapeutic Interventions against SARS-CoV-2. *Vaccines (Basel)* **9**,
553 178 (2021).
554 25. Sauer, M. M. *et al.* Structural basis for broad coronavirus neutralization. *Nat Struct Mol*
555 *Biol* **28**, 478–486 (2021).

556 26. Wec, A. Z. *et al.* Broad neutralization of SARS-related viruses by human monoclonal
557 antibodies. *Science* **369**, 731–736 (2020).
558 27. Song, G. *et al.* Cross-reactive serum and memory B-cell responses to spike protein in SARS-
559 CoV-2 and endemic coronavirus infection. *Nat Commun* **12**, 2938 (2021).
560 28. Li, W. *et al.* Structural basis and mode of action for two broadly neutralizing antibodies
561 against SARS-CoV-2 emerging variants of concern. *Cell Rep* **38**, 110210 (2022).
562 29. Hsieh, C.-L. *et al.* Stabilized coronavirus spike stem elicits a broadly protective antibody.
563 *Cell Rep* **37**, 109929 (2021).
564 30. Zhou, P. *et al.* A human antibody reveals a conserved site on beta-coronavirus spike proteins
565 and confers protection against SARS-CoV-2 infection. *Sci Transl Med* **14**, eabi9215 (2022).
566 31. Hurlburt, N. K. *et al.* Structural definition of a pan-sarbecovirus neutralizing epitope on the
567 spike S2 subunit. *Commun Biol* **5**, 342 (2022).
568 32. Pinto, D. *et al.* Broad betacoronavirus neutralization by a stem helix-specific human
569 antibody. *Science* **373**, 1109–1116 (2021).
570 33. Jennewein, M. F. *et al.* Isolation and characterization of cross-neutralizing coronavirus
571 antibodies from COVID-19+ subjects. *Cell Rep* **36**, 109353 (2021).
572 34. Iketani, S. *et al.* Antibody evasion properties of SARS-CoV-2 Omicron sublineages. *Nature*
573 **604**, 553–556 (2022).
574 35. Liu, L. *et al.* Striking antibody evasion manifested by the Omicron variant of SARS-CoV-
575 2. *Nature* **602**, 676–681 (2022).
576 36. Wang, P. *et al.* Antibody resistance of SARS-CoV-2 variants B.1.351 and B.1.1.7. *Nature*
577 **593**, 130–135 (2021).
578 37. Voss, W. N. *et al.* Prevalent, protective, and convergent IgG recognition of SARS-CoV-2
579 non-RBD spike epitopes. *Science* **372**, 1108–1112 (2021).
580 38. Du, L., Yang, Y. & Zhang, X. Neutralizing antibodies for the prevention and treatment of
581 COVID-19. *Cell Mol Immunol* **18**, 2293–2306 (2021).
582 39. Ahmed, S. *et al.* A Stabilized, Monomeric, Receptor Binding Domain Elicits High-Titer
583 Neutralizing Antibodies Against All SARS-CoV-2 Variants of Concern. *Front Immunol* **12**,
584 5214 (2021).

585 40. Bommakanti, G. *et al.* Design of an HA2-based escherichia coli expressed influenza
586 immunogen that protects mice from pathogenic challenge. *Proc Natl Acad Sci U S A* **107**,
587 13701–13706 (2010).
588 41. Mallajosyula, V. V. A. *et al.* Influenza hemagglutinin stem-fragment immunogen elicits
589 broadly neutralizing antibodies and confers heterologous protection. *Proc Natl Acad Sci U*
590 *S A* **111**, E2514–E2523 (2014).
591 42. Pallesen, J. *et al.* Immunogenicity and structures of a rationally designed prefusion MERS-
592 CoV spike antigen. *Proc Natl Acad Sci U S A* **114**, E7348–E7357 (2017).
593 43. Krarup, A. *et al.* A highly stable prefusion RSV F vaccine derived from structural analysis
594 of the fusion mechanism. *Nat Commun* **6**, 8143 (2015).
595 44. Kirchdoerfer, R. N. *et al.* Stabilized coronavirus spikes are resistant to conformational
596 changes induced by receptor recognition or proteolysis. *Sci Rep* **8**, 15701 (2018).
597 45. Wrapp, D. *et al.* Cryo-EM structure of the 2019-nCoV spike in the prefusion conformation.
598 *Science (1979)* **367**, 1260–1263 (2020).
599 46. Hsieh, C.-L. *et al.* Structure-based design of prefusion-stabilized SARS-CoV-2 spikes.
600 *Science* **369**, 1501–1505 (2020).
601 47. O'Hagan, D. T., Ott, G. S., Van Nest, G., Rappuoli, R. & Del Giudice, G. The history of
602 MF59(®) adjuvant: a phoenix that arose from the ashes. *Expert Rev Vaccines* **12**, 13–30
603 (2013).
604 48. Walls, A. C. *et al.* Elicitation of broadly protective sarbecovirus immunity by receptor-
605 binding domain nanoparticle vaccines. *Cell* **184**, 5432-5447.e16 (2021).
606 49. Cohen, A. A. *et al.* Mosaic RBD nanoparticles protect against challenge by diverse
607 sarbecoviruses in animal models. *Science* **377**, eabq0839 (2022).
608 50. Cohen, A. A. *et al.* Mosaic nanoparticles elicit cross-reactive immune responses to zoonotic
609 coronaviruses in mice. *Science* **371**, 735–741 (2021).
610 51. Ma, Y. *et al.* SARS-CoV-2 Spike Stem Protein Nanoparticles Elicited Broad ADCC and
611 Robust Neutralization against Variants in Mice. *Small* **18**, 2200836 (2022).
612 52. Ravichandran, S. *et al.* Antibody signature induced by SARS-CoV-2 spike protein
613 immunogens in rabbits. *Sci Transl Med* **12**, 3539 (2020).
614 53. Ng, K. W. *et al.* SARS-CoV-2 S2–targeted vaccination elicits broadly neutralizing
615 antibodies. *Sci Transl Med* **14**, 3715 (2022).

616 54. Weidenbacher, P. A.-B. *et al.* A ferritin-based COVID-19 nanoparticle vaccine that elicits
617 robust, durable, broad-spectrum neutralizing antisera in non-human primates. *Nat Commun*
618 **14**, 2149 (2023).
619 55. Wørzner, K. *et al.* Adjuvanted SARS-CoV-2 spike protein elicits neutralizing antibodies
620 and CD4 T cell responses after a single immunization in mice. *EBioMedicine* **63**, 103197
621 (2021).
622 56. Christensen, D. *et al.* SARS-CoV-2 spike HexaPro formulated in aluminium hydroxide and
623 administered in an accelerated vaccination schedule partially protects Syrian Hamsters
624 against viral challenge despite low neutralizing antibody responses. *Front Immunol* **14**,
625 941281 (2023).
626 57. Merkuleva, I. A. *et al.* Are Hamsters a Suitable Model for Evaluating the Immunogenicity
627 of RBD-Based Anti-COVID-19 Subunit Vaccines? *Viruses* **14**, (2022).
628 58. Sia, S. F. *et al.* Pathogenesis and transmission of SARS-CoV-2 in golden hamsters. *Nature*
629 **583**, 834–838 (2020).
630 59. Chattopadhyay, G. & Varadarajan, R. Facile measurement of protein stability and folding
631 kinetics using a nano differential scanning fluorimeter. *Protein Science* **28**, 1127–1134
632 (2019).
633 60. McCray, P. B. *et al.* Lethal Infection of K18- hACE2 Mice Infected with Severe Acute
634 Respiratory Syndrome Coronavirus . *J Virol* **81**, 813–821 (2007).
635 61. Mitchison, D. A. *et al.* A comparison of the virulence in Guinea-pigs of south indian and
636 British tubercle bacilli. *Tubercle* **41**, 1–22 (1960).
637

638 **Acknowledgments:** NM acknowledges the Prime Minister Research Fellowship for her
639 fellowship (PM/MHRD-20-17303.03). RV is a JC Bose Fellow of DST. DC acknowledges the
640 Council of Scientific and Industrial Research for his fellowship (09/079(2837)/2019-EMR-I). We
641 acknowledge Ms. Simran Srivastava for providing the sarbecoviruses spike constructs.

642 **Funding:** This work was funded in part by a grant to RV from the Bill and Melinda Gates
643 Foundation (INV-005948). Funding for infrastructural support was from DST FIST, UGC Centre
644 for Advanced study, MHRD, and the DBT IISc Partnership Program. The funders had no role in
645 study design, data collection and interpretation, or the decision to submit the work for publication.

Author contributions:

Conceptualization: RV, NM

Methodology: RV, NM, SK, RSR, RS, SBJ, MB, DC, SP, RPR, CL, VJ, PMD, AJ, SSSA

Investigation: NM, SK, RSR, RS, SBJ, NJ, MB, DC, SP, RPR, CL, VJ,

Visualization: NM, SK, RSR, RS, SBJ, NJ, MB, DC, SP, RPR, CL, VJ

Funding acquisition: RV

Project administration: RV

Supervision: RV

Writing – original draft: NM

Writing – review & editing: All authors

Competing interests: A provisional patent application has been filed for the RS2 formulations described in this manuscript. RV, NM, and RS are inventors. RV is a co-founder of Mynvax, RS, SBJ, NJ, MB, and SP are employees of Mynvax Private Limited. Other authors declare that they have no competing interests.

Data and materials availability: All data are available in the main text or the supplementary materials.

TABLES

668 **Table 1:** Kinetic parameters of RS2, S2R, and Spike for binding to different RBD conformation-
669 specific ligands in PBS pH 7.4 at 25 ºC. ND*: No dissociation.
670

Ligand	Parameter	Immunogens		
		RS2	S2R	Spike
ACE2-hFc	k_a ($M^{-1}s^{-1}$)	$2.30 \pm 0.01\times10^{5}$	$5.15 \pm 0.10\times10^{5}$	$1.07 \pm 0.01\times10^{5}$
	k_d (s^{-1})	$3.90 \pm 0.02\times10^{-4}$	$1.49 \pm 0.01\times10^{-3}$	$3.04 \pm 0.07\times10^{-5}$
	K_D (M)	$1.71 \pm 0.01\times10^{-9}$	$2.99 \pm 0.06\times10^{-9}$	$2.88 \pm 0.16\times10^{-10}$
CR3022	k_a ($M^{-1}s^{-1}$)	$3.43 \pm 0.02\times10^{5}$	$6.57 \pm 0.07\times10^{5}$	$6.17 \pm 0.11\times10^{4}$
	k_d (s^{-1})	$4.13\pm 0.03\times10^{-4}$	$1.39 \pm 0.01\times10^{-3}$	$2.45 \pm 0.05\times10^{-4}$
	K_D (M)	$1.21\pm 0.01\times10^{-9}$	$2.15 \pm 0.03\times10^{-9}$	$4.06 \pm 0.11\times10^{-9}$
S309	k_a ($M^{-1}s^{-1}$)	$5.78 \pm 0.08\times10^{4}$	$5.31 \pm 0.05\times10^{4}$	$7.61 \pm 0.13\times10^{4}$
	k_d (s^{-1})	$9.87\pm 0.26\times10^{-5}$	ND*	ND*
	K_D (M)	$1.73\pm 0.05\times10^{-9}$	ND*	ND*
ADG-2	k_a ($M^{-1}s^{-1}$)	$2.17 \pm 0.01\times10^{5}$	$2.26 \pm 0.01\times10^{5}$	$1.36 \pm 0.01\times10^{5}$
	k_d (s^{-1})	$4.51\pm 0.23\times10^{-5}$	ND*	$6.88 \pm 0.06\times10^{-5}$
	K_D (M)	$1.05\pm 0.05\times10^{-10}$	ND*	$5.10 \pm 0.20\times10^{-10}$
H014	k_a ($M^{-1}s^{-1}$)	$4.52 \pm 0.03\times10^{5}$	$7.82 \pm 0.05\times10^{5}$	$7.38 \pm 0.13\times10^{5}$
	k_d (s^{-1})	$3.49 \pm 0.03\times10^{-4}$	$1.64 \pm 0.01\times10^{-3}$	$1.66 \pm 0.05\times10^{-4}$
	K_D (M)	$7.78 \pm 0.08\times10^{-10}$	$2.14 \pm 0.03\times10^{-9}$	$2.30 \pm 0.08\times10^{-9}$

671 **Table 2:** Kinetic parameters of S2, RS2, S2R, and Spike for binding to different S2-specific ligands
672 in PBS pH 7.4 at 25 ºC. ND*: No dissociation.

673

Ligand	Parameter	Immunogens			
		RS2	S2R	Spike	S2
B6	k_a ($M^{-1}s^{-1}$)	$2.53 \pm 0.05\times10^{5}$	$1.24 \pm 0.01\times10^{5}$	$3.16 \pm 0.07\times10^{4}$	$2.04 \pm 0.07\times10^{5}$
	k_d (s^{-1})	$7.32 \pm 0.36\times10^{-4}$	$1.53 \pm 0.8\times10^{-3}$	$3.48 \pm 0.25\times10^{-5}$	$2.50 \pm 0.25\times10^{-4}$
	K_D(M)	$2.30 \pm 0.12\times10^{-9}$	$1.24 \pm 0.12\times10^{-8}$	$1.12 \pm 0.08\times10^{-9}$	$1.22 \pm 0.08\times10^{-9}$
CC40.8	k_a ($M^{-1}s^{-1}$)	$1.62 \pm 0.01\times10^{5}$	$1.62 \pm 0.02\times10^{5}$	$1.19 \pm 0.02\times10^{5}$	9.11×10^{4}
	k_d (s^{-1})	$6.77 \pm 0.01\times10^{-4}$	$5.30 \pm 1.6\times10^{-4}$	ND*	ND*
	K_D (M)	$4.22 \pm 0.08\times10^{-9}$	$3.23 \pm 0.03\times10^{-9}$	ND*	ND*

674

675

676 **Table 3:** Kinetic parameters for binding of lyophilized and resolubilized RS2 after incubation of
677 lyophilized protein at 37 °C for 1 month, to different RBD-specific and S2-specific ligands in PBS
678 pH 7.4 at 25 ºC. ND*: No dissociation.

679

680

Ligand	**k_a ($M^{-1}s^{-1}$)**	**k_d (s^{-1})**	**K_D (M)**
ACE-2hFc	$1.2 \pm 0.01\times10^{5}$	$3.2 \pm 0.01\times10^{-4}$	$2.7 \pm 0.01\times10^{-9}$
CR3022	$4.8 \pm 0.01\times10^{5}$	$7.9 \pm 0.4\times10^{-4}$	$1.6 \pm 0.01\times10^{-9}$
S309	$1.2 \pm 0.01\times10^{5}$	$3.2 \pm 0.01\times10^{-5}$	$2.4 \pm 0.01\times10^{-10}$
H014	$5.0 \pm 0.01\times10^{5}$	$6.8 \pm 0.4\times10^{-4}$	$1.3 \pm 0.01\times10^{-9}$
B6	$1.1 \pm 0.01\times10^{5}$	$1.6 \pm 0.01\times10^{-5}$	$1.2 \pm 0.01\times10^{-10}$
CC40.8	$1.1 \pm 0.01\times10^{5}$	ND*	ND*

681 **Figure Legends**

682 **Fig. 1**. **Characterization of S2, RS2, S2R, and Spike immunogens. (A)** Schematic
683 representation of designed immunogen sequences. **(B)** Reducing SDS-PAGE profile of protein
684 samples. **(C-F)** SEC profile of purified **(C)** S2, **(D)** RS2, **(E)** S2R and **(F)** Spike immunogens.

685

686 **Fig. 2. Equilibrium thermal unfolding, transient thermal stability and limited trypsin**
687 **proteolytic profiles of designed immunogens. (A-D)** Thermal unfolding profiles. Apparent
688 melting temperature of **(A)** RS2, **(B)** S2R, **(C)** S2 and **(D)** Spike were measured using Nano-DSF.
689 **(E-H)** Transient thermal stability profiles. Protein samples were subjected to different
690 temperatures (4, 37, and 50 °C) for one hour. Thermal stability of **(E)** RS2, **(F)** S2R, **(G)** S2 and
691 **(H)** Spike was monitored using Nano-DSF. Normalized first derivative of fluorescence at 350 nm
692 is plotted as function of temperature. **(I-L)** Proteolytic stability profile. Coomassie stained SDS-
693 PAGE profiles of purified **(I)** RS2, **(J)** S2R, **(K)** S2 and **(L)** Spike subjected to TPCK-Trypsin
694 proteolysis at 37 °C and 4 °C.

695 **Fig 3. Immunogenicity of RBD, S2 and S2R in hACE-2 expressing mice.** Three groups of
696 hACE-2 expressing transgenic mice were primed and boosted with 2µg of RBD, S2 and S2R
697 respectively, followed by an intranasal challenge with 10^5 pfu of the beta variant of SARS-CoV-
698 2. **(A-C)** ELISA endpoint titers against RBD, S2, and spike ectodomain respectively two weeks
699 post-boost. **(D and E)** Neutralizing antibody titers elicited by RBD, S2, and S2R against B.1 and
700 BA.1 Omicron SARS-CoV-2 pseudovirus. No neutralization was seen with S2 immunized
701 animals. **(F)** Neutralizing antibody titers elicited by S2R against various pseudoviruses. Lines
702 connect the neutralizing titers for different variants in a sera sample from an individual animal
703 against different variants. **(G)** Neutralization curves of pooled S2 immunized mice sera, MAb
704 S309, and S2 immunized mice sera in presence of S309. The sera sample was tested in five
705 technical repeats. Each point represents the median of five independent values. **(H)** Survival
706 Curve. **(I)** Average weight changes up to 5 days post-challenge. **(J)** Lung viral titer. **(K)**
707 Histopathology scores of lungs. **(L)** Histology of lung tissue sections from unimmunized-
708 unchallenged control (UC), unimmunized- Beta variant challenged control (Unimmunized-Beta)
709 and mice immunized with RBD, S2 and S2R at 4X magnification. Titers are shown as geometric

710 mean with geometric SD. The ELISA binding, neutralization titer, lung viral titer and
711 histopathology score data were analyzed with a two-tailed Mann–Whitney test and non-parametric
712 Kruskal-Wallis test with Dunn's multiple correction. Pairwise weight changes were analyzed with
713 a Multiple Student's t-test with Bonferroni Dunn's correction method. (ns indicates non-
714 significant, * indicates $p < 0.05$, ** indicates $p < 0.01$, **** indicates $p < 0.0001$).

715

716 **Fig. 4. Immunogenicity of RS2 and Spike in BALB/c mice.** BALB/c mice were immunized
717 twice with either 2µg RS2 or 2µg Spike, followed by intranasal challenge with 10^5 pfu of MA-10
718 mouse adapted SARS-CoV-2. Two weeks following the boost, RBD, S2 and Spike specific IgG
719 and neutralizing titers in immunized mice sera were measured **(A-C)** ELISA endpoint titers against
720 RBD, S2 and spike ectodomain, respectively. **(D-K)** Comparison of neutralizing antibody titers
721 elicited by 2µg of RS2 and Spike against **(D)** B.1, **(E)** Beta, **(F)** Delta, **(G)** BA.1, **(H)** BA.5, **(I)**
722 BF.7, **(J)** WIV-1, and **(K)** SARS-CoV-1 pseudoviruses. **(L)** Average weight changes upto six days
723 post-MA10 challenge. **(M)** Lung viral titers **(N)** Histopathology scores of lungs. **(O)** Histology of
724 lung tissue sections from unimmunized-unchallenged control (UC), Unimmunized-MA10 virus
725 challenged control (Unimmunized MA-10), mice immunized with Spike or RS2 at 4X
726 magnification. Titers are shown as geometric mean with geometric SD. The ELISA binding,
727 neutralization titer, lung viral titer, and histopathology score data were analyzed with a two-tailed
728 Mann–Whitney test. Pairwise weight changes were analyzed with a Multiple Student's t-test with
729 Bonferroni Dunn's correction method. (ns indicates non-significant, * indicates $p < 0.05$, **
730 indicates $p < 0.01$, **** indicates $p < 0.0001$).

731 **Fig. 5. Stability of RS2.** Characterization of lyophilized and resolubilized RS2 after incubation at
732 37 °C for 1 month. **(A-H)** Physiochemical characterization of RS2 in 1X PBS with equal amount
733 (v/v) of SWE adjuvant incubated at 5 and 40 °C in polypropylene (PP) and glass vials (GV) for
734 one month. Adjuvant properties were measured on day 0, day 7, day 14 and day 30. **(A)** Particle
735 size, **(B)** Polydispersity Index, **(C)** Zeta Potential, **(D)** pH, **(E)** Osmolality, **(F)** Squalene content.
736 **(G and H)** Antigenic integrity of RS2 in PBS and SWE adjuvant was measured based on binding
737 to CR3022 using ELISA. **(I)** Day 7, **(J)** Day 14, **(K)** Day 30. Freshly thawed RS2 sample without
738 any external modification 'RS2 ctrl extemp' was used as a control for undegraded antigen.

739 **Fig. 6. Immunogenicity of lyophilized RS2, that had been incubated at 37 °C for 1 month, in**
740 **hACE-2 expressing transgenic mice.** hACE-2 expressing transgenic mice immunized twice with
741 20µg of lyophilized RS2 that was previously incubated at 37°C for over a month and then
742 formulated in SWE adjuvant. This was followed by intranasal challenge with 10^4 pfu Beta and
743 Delta variants. **(A)** ELISA endpoint titers against RBD, S2, and spike ectodomain. **(B)** Neutralizing
744 antibody titers against B.1, Beta, Delta and BA.1 pseudoviruses. **(C)** Neutralizing antibody titers
745 elicited by lyophilized RS2 subjected to 37°C for over a month (Lyo) and non-lyophilized RS2
746 (Non-lyo) stored at 4 °C against B.1 and BA.1 Omicron SARS-CoV-2 pseudovirus **(D and E)**
747 Average weight change upto nine days post-Beta and Delta virus challenge respectively. **(F)**
748 Survival curve. **(G and H)** Lung viral titers in RS2 immunized mice, challenged with Beta VOC
749 and Delta VOC respectively. **(I and J)** Histopathology scores of lungs. **(K)** Histology of lung
750 tissue sections from unimmunized-unchallenged control (UC), mice immunized with 20µg RS2
751 challenged with Beta variants (RS2-Beta challenged), unimmunized Delta virus challenged control
752 (Unimmunized-Delta), mice immunized with 20µg RS2 and challenged with Delta variant (RS2-
753 Delta challenged), at 4X magnification. None of the unimmunized controls survived the Beta virus
754 challenge (Unimmunized-Beta). Titers are shown as geometric mean with geometric SD. The
755 ELISA binding, neutralization titer, lung viral titer and histopathology score data were analyzed
756 with a two-tailed Mann–Whitney test and non-parametric Kruskal-Wallis test with Dunn's
757 multiple correction. Pairwise weight changes were analyzed with a Multiple Student's t-test with
758 Bonferroni Dunn's correction method. (ns indicates non-significant, * indicates $p < 0.05$, **
759 indicates $p < 0.01$, **** indicates $p < 0.0001$).

760 **Fig. 7. Comparative protective efficacy of RS2 and spike in hamsters.** Syrian hamsters were
761 immunized twice with 5µg of RS2 or Spike, followed by intranasal challenge with 10^5 pfu of
762 the Beta VOC. **(A-C)** ELISA endpoint titers against RBD, S2 and spike ectodomain, respectively.
763 **(D-K)** Comparative neutralizing antibody titers elicited by 5µg of RS2 and spike against **(D)** B.1,
764 **(E)** Beta, **(F)** Delta, **(G)** BA.1, **(H)** BA.5, **(I)** BF.7, **(J)** WIV-1 and , **(K)** SARS-CoV-1 pseudovirus.
765 **(L)** Average weight change upto five days post-beta variant virus challenge. **(M)** Lung viral titers
766 **(N)** Histology of lung tissue sections from unimmunized-unchallenged control (UC),
767 unimmunized-Beta challenged control (Unimmunized-Beta) and hamsters immunized with Spike
768 and RS2 at 4X magnification. **(O)** Histopathology scores of lungs. The ELISA binding,

769 neutralization titer, lung viral titer and, histopathology score data were analyzed with a two-tailed
770 Mann–Whitney test. Pairwise weight changes were analyzed with a Multiple Student's t-test with
771 Bonferroni Dunn's correction method. (ns indicates non-significant, * indicates $p < 0.05$, **
772 indicates $p < 0.01$, **** indicates $p < 0.0001$).

773 **Supplementary Figure Legends**

774 **Fig. S1. Comparative immunogenicity of RS2 and S2R in mice.** BALB/c were mice immunized
775 twice with 20µg of RS2 or S2R. Two weeks following boost vaccination RBD and Spike specific
776 IgG levels and neutralizing titers were measured in immunized mice sera samples. Comparative
777 ELISA endpoint titers against **(A)** RBD and **(B)** Spike ectodomain, respectively **(C and D)**
778 Comparative neutralizing antibody titers elicited by 20µg of RS2 and S2R against **(C)** B.1, **(D)**
779 Delta variant pseudoviruses. Titers are shown as geometric mean with geometric SD. The ELISA
780 binding and neutralization titers were analyzed with a two-tailed Mann–Whitney test. (ns indicates
781 non-significant, * indicates $p < 0.05$, ** indicates $p < 0.01$, **** indicates $p < 0.0001$).
782

783 **Fig. S2. Effect of transient thermal stress on lyophilized RS2.** RS2 protein was dialyzed in
784 water and then lyophilized. **(A)** Equilibrium thermal unfolding profile of RS2 before and after
785 lyophilization and resolubilization in PBS. Lyophilized RS2 was incubated for one hour at
786 different temperatures (4, 37, 50, 70 and 90°C). Following reconstitution in PBS buffer, thermal
787 stability of **(B)** RS2 was monitored using Nano-DSF. **(C)** Thermal stability of lyophilized and
788 resolubilized RS2 after incubation at 37 °C for 1 month. **(D-H)** In addition, RS2 samples were
789 characterized for binding of with panel of RBD **(D-F)** and S2 **(G and H)** specific antibodies using
790 SPR **(D)** ACE2-hFc, **(E)** CR3022, **(F)** S309, **(G)** CC40.8, and **(H)** B6.
791

792 **Fig. S3. Competition of immunized mice sera with RBD and S2 specific monoclonal**
793 **antibodies.** BALB/c mice were immunized with 20µg of RBD, Spike, or RS2. Top panel:
794 Schematic of assay. Bottom panel **(A and B)** ELISA competition titers against **(A)** S2X259 (Class
795 4) and **(B)** B6 (S2 helix) monoclonal antibodies for individual, immunized mice sera. Immunogens
796 used to elicit respective sera are listed on the x-axis and competition titers on the y-axis of each
797 bar graph.
798

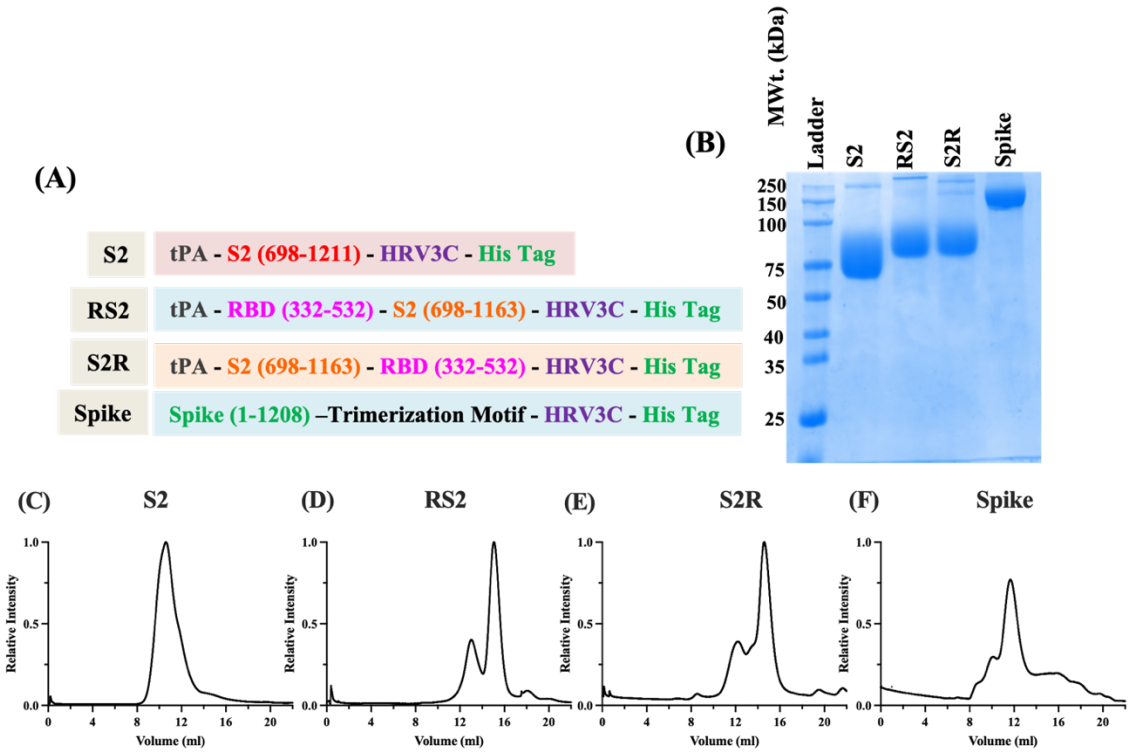
(A)
S2
tPA - S2 (698-1211) - HRV3C - His Tag
RS2
tPA - RBD (332-532) - S2 (698-1163) - HRV3C - His Tag
S2R
tPA - S2 (698-1163) - RBD (332-532) - HRV3C - His Tag
Spike
Spike (1-1208) –Trimerization Motif - HRV3C - His Tag
(B)
MWt. (kDa)
Ladder
S2
RS2
S2R
Spike
250
150
100
75
50
40
35
25
(C)
S2
(D)
RS2
(E)
S2R
(F)
Spike
Relative Intensity
Volume (ml)

Fig. 1.

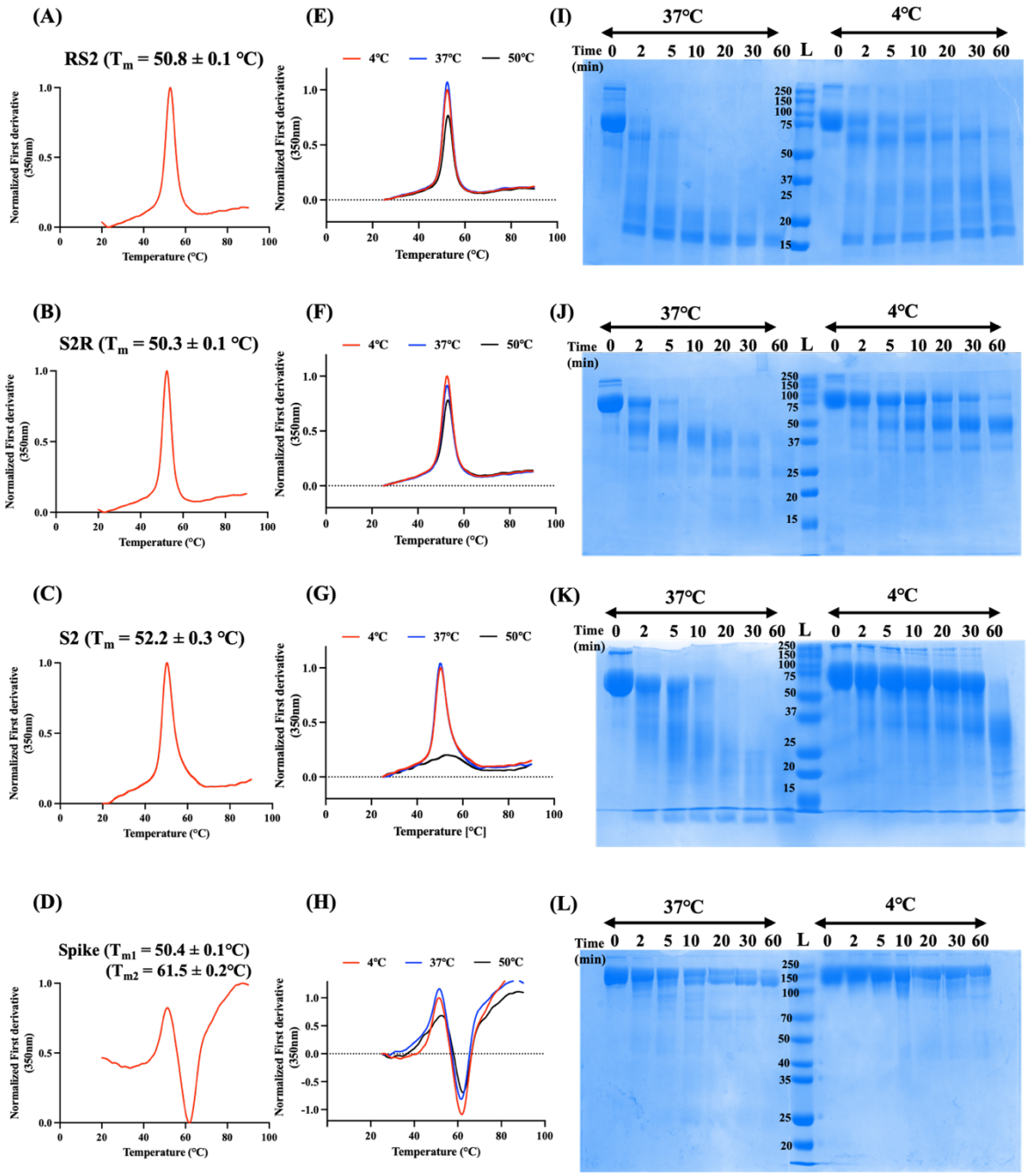
(A)
RS2 (T_m = 50.8 ± 0.1 °C)
(B)
S2R (T_m = 50.3 ± 0.1 °C)
(C)
S2 (T_m = 52.2 ± 0.3 °C)
(D)
Spike (T_{m1} = 50.4 ± 0.1°C)
(T_{m2} = 61.5 ± 0.2°C)
Normalized First derivative (350nm)
Temperature (°C)
(E)
(F)
(G)
(H)
4°C
37°C
50°C
Temperature [°C]
(I)
(J)
(K)
(L)
37°C
4°C
Time (min)
0 2 5 10 20 30 60 L 0 2 5 10 20 30 60

Fig. 2.

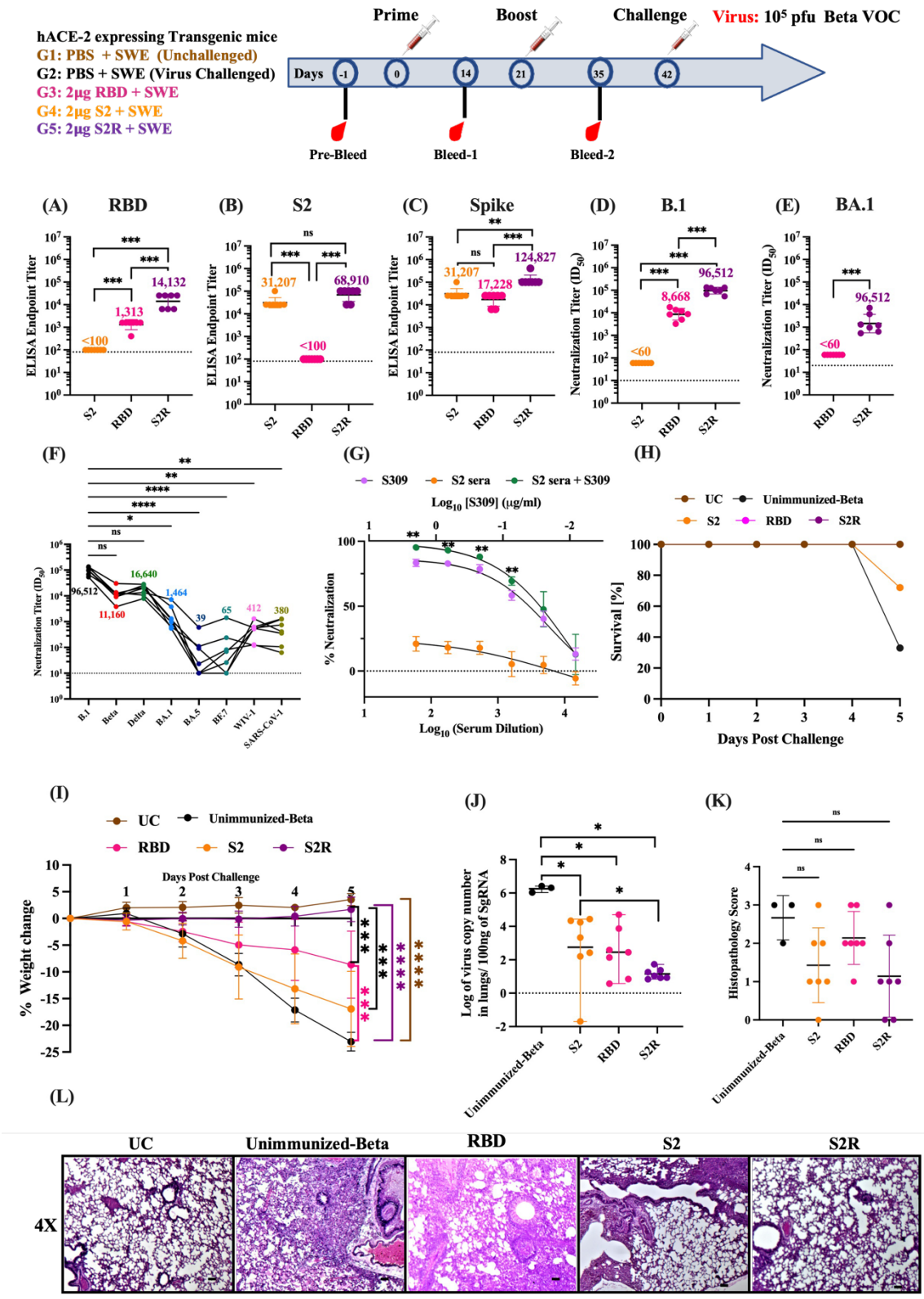
hACE-2 expressing Transgenic mice
G1: PBS + SWE (Unchallenged)
G2: PBS + SWE (Virus Challenged)
G3: 2µg RBD + SWE
G4: 2µg S2 + SWE
G5: 2µg S2R + SWE
Prime
Boost
Challenge
Virus: 10^5 pfu Beta VOC
Days
Pre-Bleed
Bleed-1
Bleed-2
(A) RBD
(B) S2
(C) Spike
(D) B.1
(E) BA.1
ELISA Endpoint Titer
Neutralization Titer (ID50)
(F)
(G)
(H)
S309
S2 sera
S2 sera + S309
% Neutralization
Survival [%]
Days Post Challenge
(I)
UC
Unimmunized-Beta
RBD
S2
S2R
% Weight change
(J)
Log of virus copy number in lungs/ 100ng of SgRNA
(K)
Histopathology Score
(L)
4X

Fig. 3

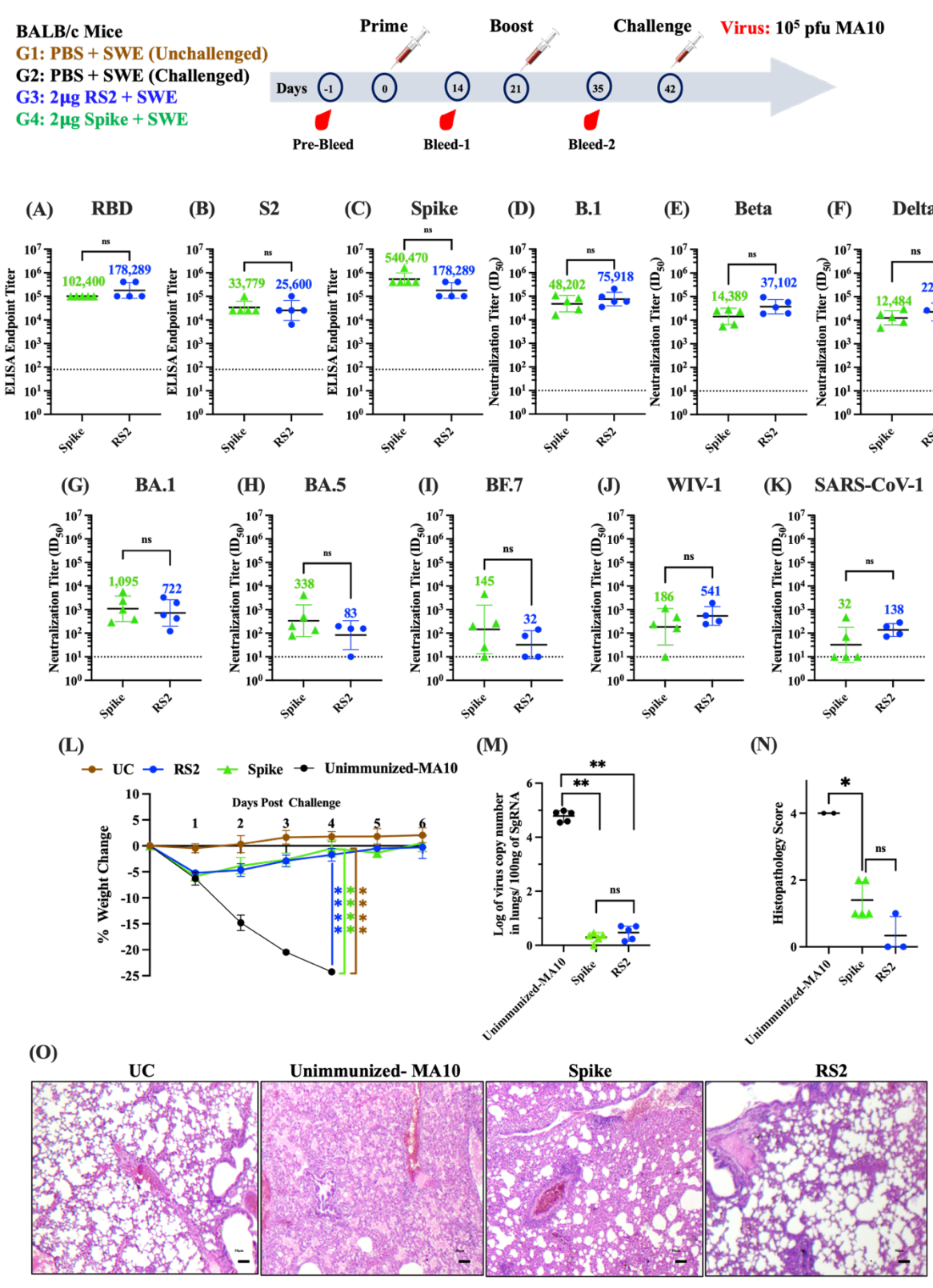
BALB/c Mice
G1: PBS + SWE (Unchallenged)
G2: PBS + SWE (Challenged)
G3: 2µg RS2 + SWE
G4: 2µg Spike + SWE
Prime
Boost
Challenge
Virus: 10^5 pfu MA10
Days
-1
0
14
21
35
42
Pre-Bleed
Bleed-1
Bleed-2
(A) RBD
(B) S2
(C) Spike
(D) B.1
(E) Beta
(F) Delta
ELISA Endpoint Titer
Neutralization Titer (ID50)
ns
102,400
178,289
33,779
25,600
540,470
178,289
48,202
75,918
14,389
37,102
12,484
22,529
Spike
RS2
(G) BA.1
(H) BA.5
(I) BF.7
(J) WIV-1
(K) SARS-CoV-1
1,095
722
338
83
145
32
186
541
32
138
(L)
UC
RS2
Spike
Unimmunized-MA10
Days Post Challenge
% Weight Change
(M)
Log of virus copy number in lungs/ 100ng of SgRNA
**
ns
Unimmunized-MA10
Spike
RS2
(N)
Histopathology Score
*
ns
(O)
UC
Unimmunized- MA10
Spike
RS2

Fig. 4.

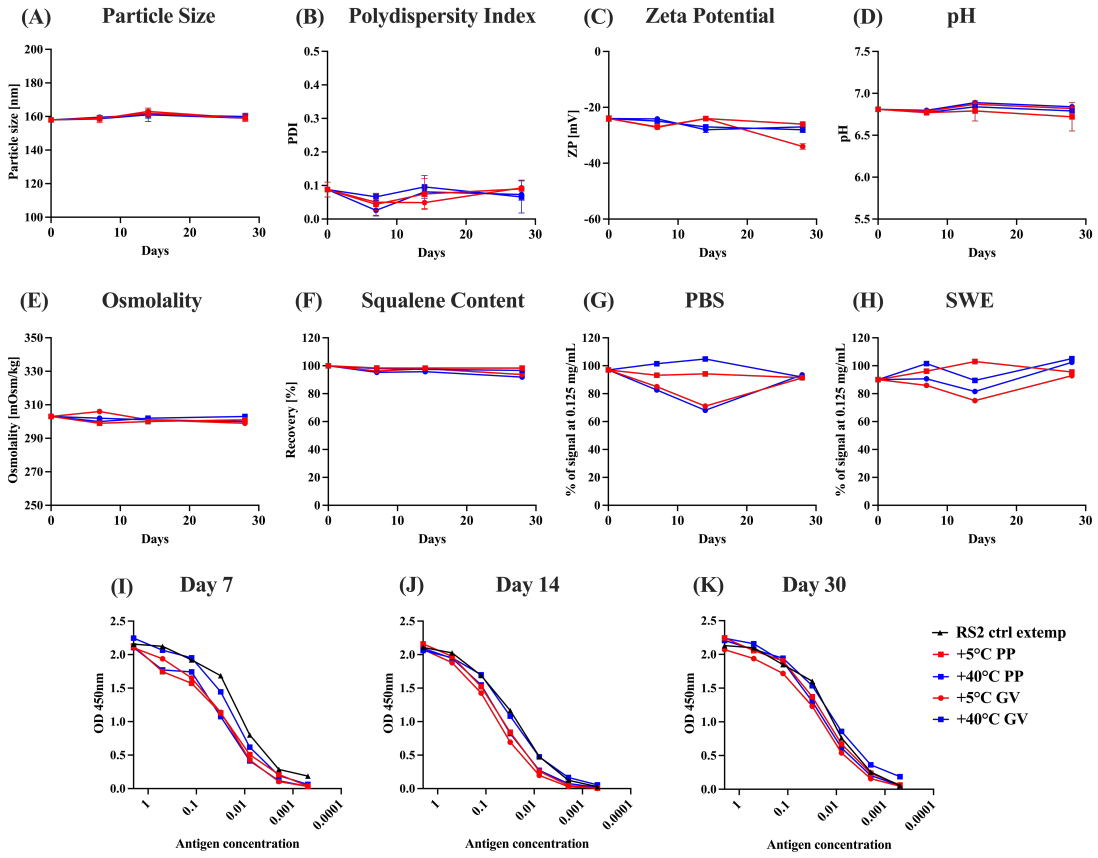
(A) Particle Size
Particle size [nm]
Days
(B) Polydispersity Index
PDI
Days
(C) Zeta Potential
ZP [mV]
Days
(D) pH
pH
Days
(E) Osmolality
Osmolality [mOsm/kg]
Days
(F) Squalene Content
Recovery [%]
Days
(G) PBS
% of signal at 0.125 mg/mL
Days
(H) SWE
% of signal at 0.125 mg/mL
Days
(I) Day 7
(J) Day 14
(K) Day 30
OD 450nm
Antigen concentration
RS2 ctrl extemp
+5°C PP
+40°C PP
+5°C GV
+40°C GV

Fig. 5.

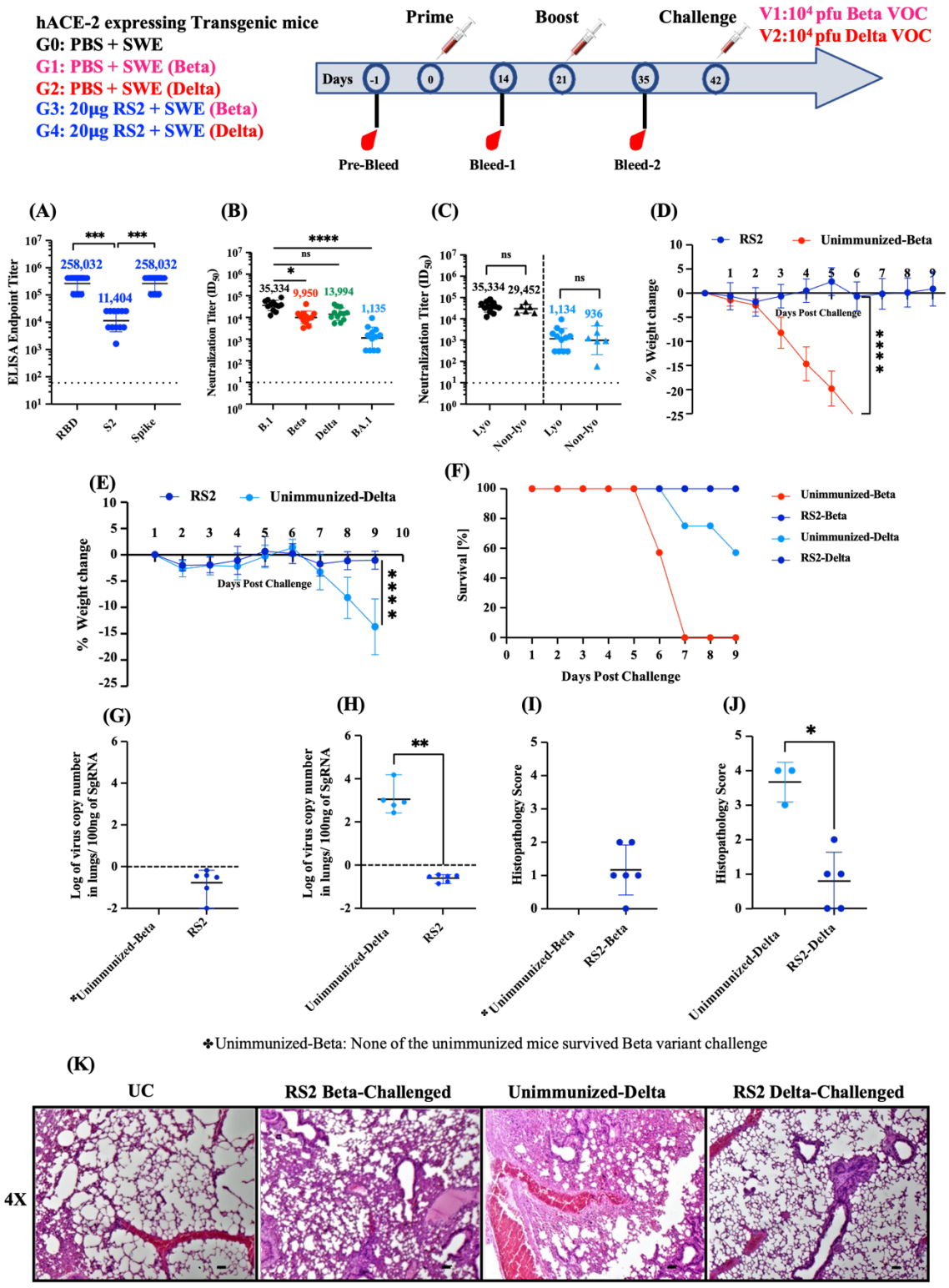
hACE-2 expressing Transgenic mice
G0: PBS + SWE
G1: PBS + SWE (Beta)
G2: PBS + SWE (Delta)
G3: 20µg RS2 + SWE (Beta)
G4: 20µg RS2 + SWE (Delta)
Prime
Boost
Challenge
V1:10⁴ pfu Beta VOC
V2:10⁴ pfu Delta VOC
Days
-1
0
14
21
35
42
Pre-Bleed
Bleed-1
Bleed-2
(A)
ELISA Endpoint Titer
258,032
11,404
258,032
RBD
S2
Spike
(B)
Neutralization Titer (ID50)
35,334
9,950
13,994
1,135
B.1
Beta
Delta
BA.1
(C)
Neutralization Titer (ID50)
35,334
29,452
1,134
936
Lyo
Non-lyo
(D)
RS2
Unimmunized-Beta
% Weight change
Days Post Challenge
(E)
RS2
Unimmunized-Delta
% Weight change
Days Post Challenge
(F)
Survival [%]
Days Post Challenge
Unimmunized-Beta
RS2-Beta
Unimmunized-Delta
RS2-Delta
(G)
Log of virus copy number in lungs/ 100ng of SgRNA
*Unimmunized-Beta
RS2
(H)
Log of virus copy number in lungs/ 100ng of SgRNA
Unimmunized-Delta
RS2
(I)
Histopathology Score
*Unimmunized-Beta
RS2-Beta
(J)
Histopathology Score
Unimmunized-Delta
RS2-Delta
✤Unimmunized-Beta: None of the unimmunized mice survived Beta variant challenge
(K)
UC
RS2 Beta-Challenged
Unimmunized-Delta
RS2 Delta-Challenged
4X

Fig. 6.

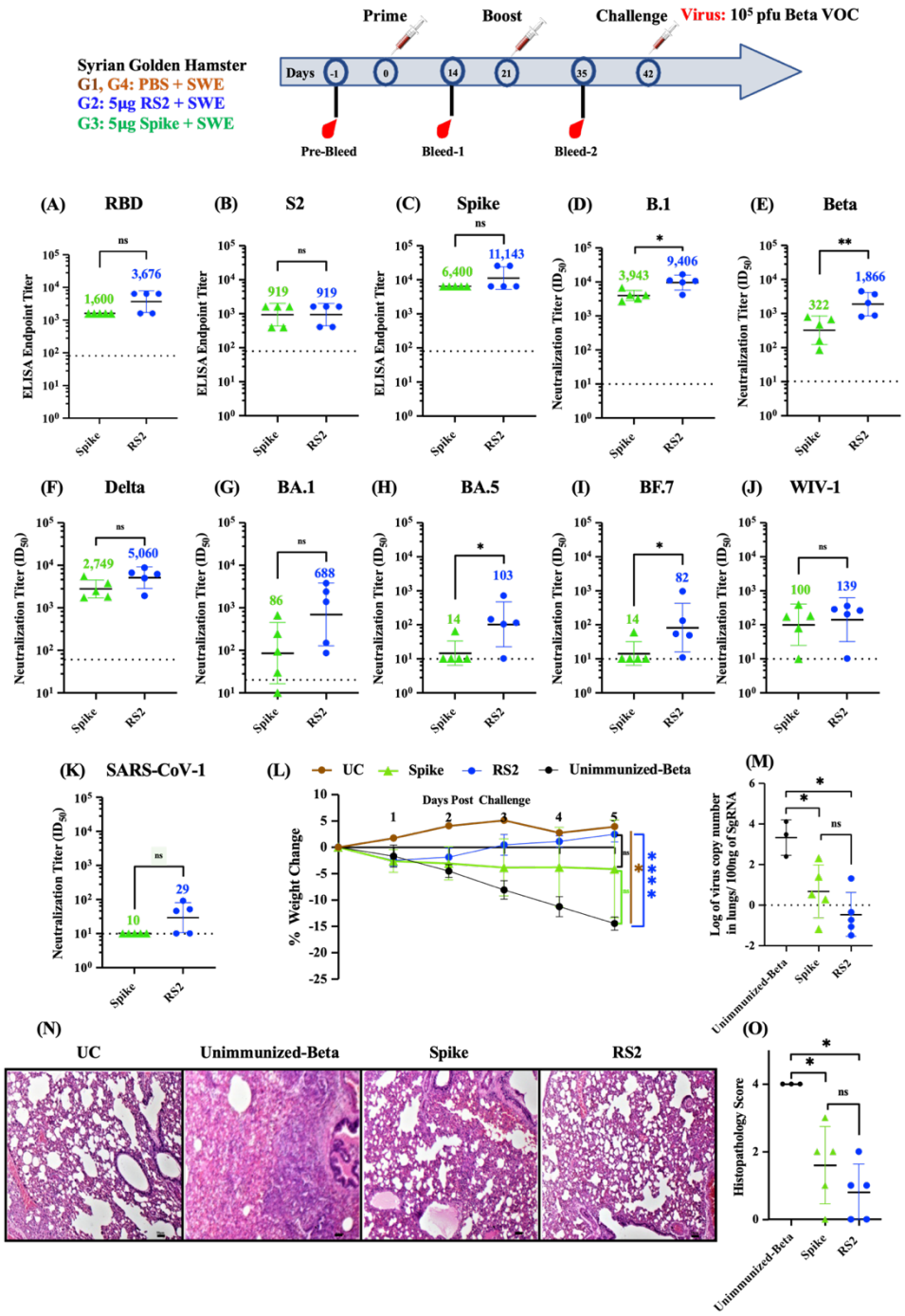
Prime
Boost
Challenge
Virus: 10⁵ pfu Beta VOC
Syrian Golden Hamster
G1, G4: PBS + SWE
G2: 5µg RS2 + SWE
G3: 5µg Spike + SWE
Days
-1
0
14
21
35
42
Pre-Bleed
Bleed-1
Bleed-2
(A) RBD
(B) S2
(C) Spike
(D) B.1
(E) Beta
(F) Delta
(G) BA.1
(H) BA.5
(I) BF.7
(J) WIV-1
(K) SARS-CoV-1
(L)
UC
Spike
RS2
Unimmunized-Beta
Days Post Challenge
% Weight Change
(M)
Log of virus copy number in lungs/ 100mg of SgRNA
(N)
UC
Unimmunized-Beta
Spike
RS2
(O)
Histopathology Score
ELISA Endpoint Titer
Neutralization Titer (ID50)
ns
1,600
3,676
919
919
6,400
11,143
3,943
9,406
322
1,866
2,749
5,060
86
688
14
103
14
82
100
139
10
29

Fig. 7.

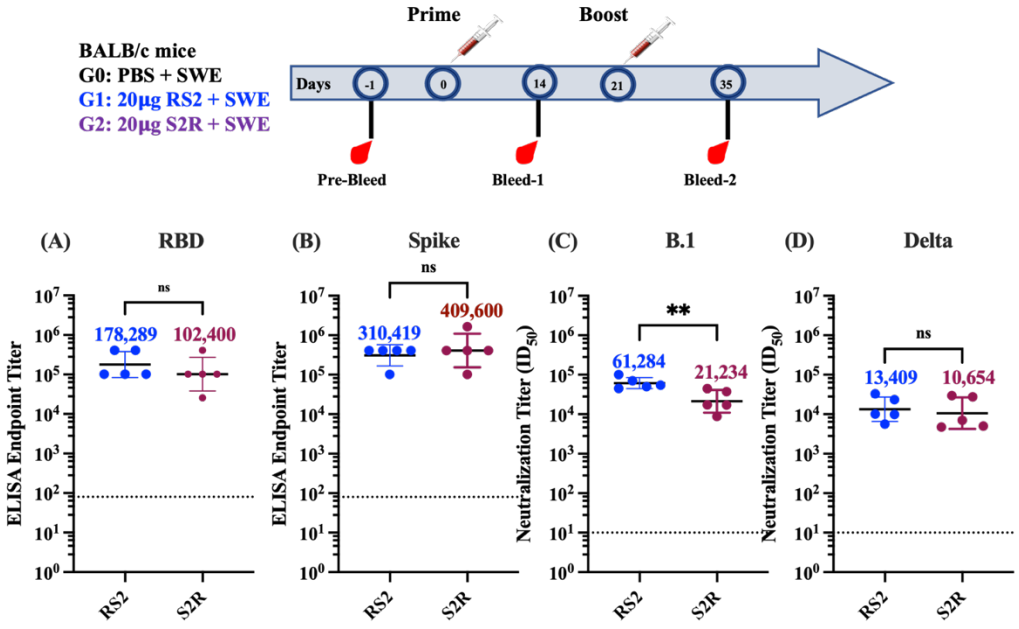
BALB/c mice
G0: PBS + SWE
G1: 20µg RS2 + SWE
G2: 20µg S2R + SWE
Prime
Boost
Days
-1
0
14
21
35
Pre-Bleed
Bleed-1
Bleed-2
(A) RBD
(B) Spike
(C) B.1
(D) Delta
ELISA Endpoint Titer
Neutralization Titer (ID50)
ns
**
178,289
102,400
310,419
409,600
61,284
21,234
13,409
10,654
RS2
S2R

Fig. S1.

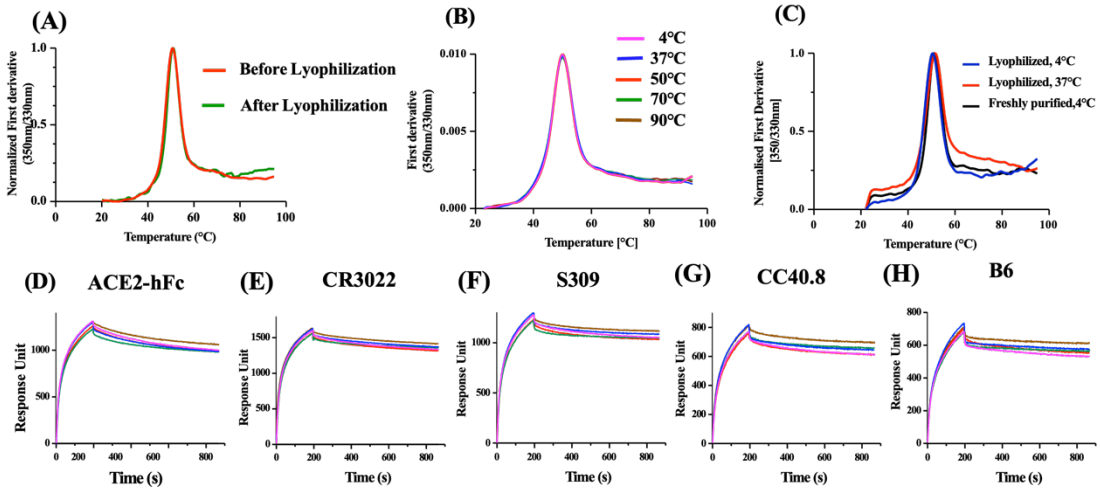
(A)
Before Lyophilization
After Lyophilization
Normalized First derivative (350nm/330nm)
Temperature (°C)
(B)
4°C
37°C
50°C
70°C
90°C
First derivative (350nm/330nm)
Temperature [°C]
(C)
Lyophilized, 4°C
Lyophilized, 37°C
Freshly purified,4°C
Normalised First Derivative [350/330nm]
Temperature (°C)
(D) ACE2-hFc
(E) CR3022
(F) S309
(G) CC40.8
(H) B6
Response Unit
Time (s)

Fig. S2.

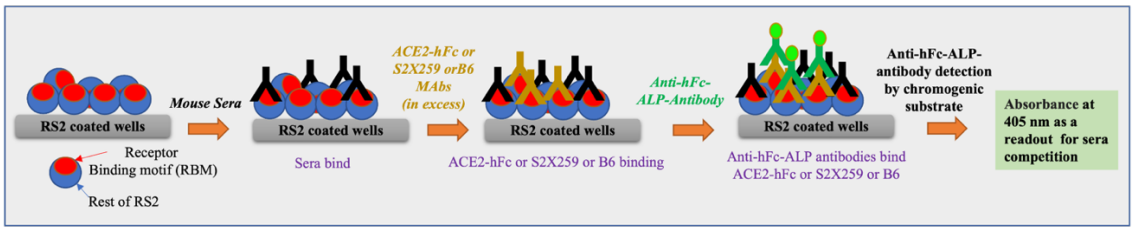
RS2 coated wells
Receptor
Binding motif (RBM)
Rest of RS2
Mouse Sera
RS2 coated wells
Sera bind
ACE2-hFc or
S2X259 orB6
MAbs
(in excess)
RS2 coated wells
ACE2-hFc or S2X259 or B6 binding
Anti-hFc-
ALP-Antibody
RS2 coated wells
Anti-hFc-ALP antibodies bind
ACE2-hFc or S2X259 or B6
Anti-hFc-ALP-
antibody detection
by chromogenic
substrate
Absorbance at
405 nm as a
readout for sera
competition

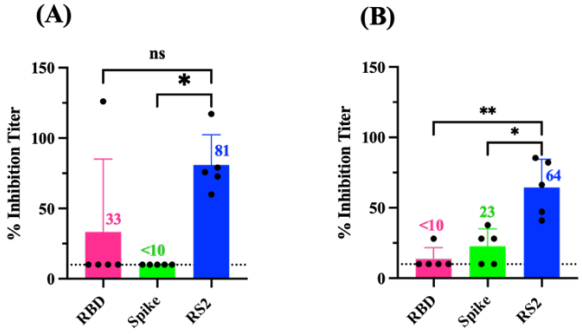
(A)
(B)
% Inhibition Titer
150
100
50
0
ns
*
**
33
<10
81
<10
23
64
RBD
Spike
RS2

Fig. S3.